

SLAC-PUB-997
CO-3067(2)-1
(TH)
December 1971

SCALING PROPERTIES AND THE BOUND-STATE NATURE
OF THE PHYSICAL NUCLEON

S. D. Drell

SLAC, Stanford University, Stanford, California 94305

and

T. D. Lee

Columbia University, New York, N. Y. 10027

(Submitted to Phys. Rev.)

This research was supported in part by the U. S. Atomic Energy Commission.

ABSTRACT

The scaling property in deep inelastic electron scattering is established by regarding the physical nucleon as a bound state of a bare nucleon and a bare meson (or a few bare mesons). This bound-state formulation provides a fully relativistic generalization of the "parton" model that is no longer restricted to infinite momentum frames. It also connects the scaling property in inelastic processes with the rapid decrease of the electromagnetic form factors in elastic scattering. Rigorous statements are derived for specific bound-state solutions of the Bethe-Salpeter equation with the ladder approximation. An Adler sum rule is derived and crossing properties are discussed.

A general phenomenological approach is developed which is relativistically covariant and gauge invariant, and which allows one to correlate directly the observed structure functions and form factors with the appropriate bound-state wave function. If all constituents in the bound state are assumed to be of masses $\lesssim 1 \text{ GeV}$, the model gives a qualitative understanding as to why the scaling property is experimentally observed at relatively moderate energies.

I. Introduction

While the validity of the scaling hypothesis¹ has been well-established by recent extensive experimental investigations on inelastic electron-proton scattering², its theoretical basis remains in an unsatisfactory state. The original parton idea of Feynman puts a special emphasis on the infinite-momentum frame of reference. It is suggested that in the infinite-momentum frame, the electromagnetic property of the assumed pointlike constituents of the physical nucleon can be treated as that of an assembly of independent free particles. The "infinite momentum frame", by itself, is clearly not a Lorentz invariant concept. Furthermore, one can easily show³ that, in general, the direction of the infinite momentum cannot be arbitrary. It must be limited to a certain restrictive set of directions, depending on the virtual photon momentum; otherwise, the mass of each of the pointlike constituents has to be lighter than that of the physical proton, and that would be too unphysical. Naturally, this leads to questions of whether such an ad hoc rule can be derived from a relativistically invariant theory.

In the literature, there have been several attempts to try to derive the scaling property from the usual relativistic local field theory. So far, the only success has been limited to either the trivial case of free particles (free except for their electromagnetic interaction), or the unphysical case of a super-renormalizable ϕ^3 -type theory⁴ in which all particles must be of zero spin. For the physically interesting case of spin $\frac{1}{2}$ charged particles with some non-electromagnetic interaction, straightforward calculation in lowest order perturbative expansions leads to a logarithmic deviation from scaling

behavior⁵. In order to derive scaling properties for such field theories with renormalizable but not super-renormalizable hadronic interactions, it has been necessary to introduce additional ad hoc rules, such as either a transverse momentum cut-off⁶ or the so-called "formal manipulation" of current operators⁷, etc. However, at present the theoretical foundation of such rules appears to be quite uncertain. In particular, the transverse momentum cut-off in the field theoretical derivation of scaling leads to a formalism and a scattering amplitude that are current-conserving only in the infinite momentum frame and in the scaling region. Therefore, it is difficult to see how one may derive such an ad hoc cut-off procedure in a bona fide relativistic field theory.

The purpose of this paper is to point out that if one regards the physical nucleon as a bound state, then there exists a large class of relativistic field theories in which, at least for the deep inelastic electron-nucleon scattering, the scaling property as well as the approach to scaling can be derived by using the conventional field-theoretical rules for bound states, provided radiative corrections are neglected⁸. In constructing the explicit bound-state wave function for the physical nucleon, there is, of course, a certain degree of arbitrariness with respect to both the nature of its constituents and that of the binding forces. In view of the experimental fact that the scaling limit seems to occur at a remarkably low energy range, it seems reasonable that the masses of the constituents and the relevant binding energy should all lie approximately in the 1 GeV range. Therefore, at least in terms of quantum numbers, these constituents should more closely resemble known particles than any unknown particles, such as quarks⁹. As a first example, we assume in section II that the physical nucleon is simply a two-body bound state composed of a "bare" nucleon of spin $\frac{1}{2}$ and a "bare" meson of

spin 0. The various quantum numbers (charge, spin, isospin, etc.) of the "bare" nucleon are assumed to be the same as those of the physical nucleon; for simplicity, we may assume its mass to be the same as, or at least comparable to, the physical nucleon mass. Similarly, for reasons of simplicity, the "bare" meson is assumed to be an SU_3 singlet, and its mass as well as other quantum numbers to be the same as those of the physical X^0 meson. There is, however, an important difference between a "bare" particle and the corresponding "physical" one. The electromagnetic form factors of a "bare" particle are always assumed to be independent of the 4-momentum transfer. In the language of the parton model, these "bare" particles are the "pointlike" constituents of the physical nucleon. Whether or not such pointlike "bare" particles that are introduced as constituents of a physical nucleon will ever be observed is an open question—as is also the case for "quarks"—at this time. [See, however, the discussion given in section V below.]

To illustrate the relation between the scaling limit and the conventional field-theoretical rules for the bound state, we adopt the Bethe-Salpeter equation with the ladder approximation. The covariant potential responsible for the binding is assumed to be of the general form

$$V(q) = \int \frac{\sigma(\kappa^2) d\kappa^2}{q^2 + \kappa^2} \quad (1.1)$$

where q^2 denotes the square of the 4-momentum transfer. The integral $\int \sigma(\kappa^2) d\kappa^2$ is assumed to be convergent; thus,

$$V(q) \sim 0(q^{-2}) \quad \text{as } q^2 \rightarrow \infty. \quad (1.2)$$

As will be shown, this implies that as the relative momentum k between the two "bare"

particles in the bound state approaches infinity, the wave function $\phi(k)$ of the Bethe-Salpeter equation has a similar asymptotic behavior¹⁰; i.e.,

$$\phi(k) \sim O(k^{-2}) \quad \text{as } k^2 \rightarrow \infty. \quad (1.3)$$

By using this asymptotic property, one can then establish the existence of the scaling limit for the bound-state solution. The underlying picture for deep inelastic electron scattering that emerges provides a fully relativistic generalization of the "parton" model that is no longer restricted to special infinite momentum frames. It will be demonstrated that one may view the dynamic process as simply the physical proton dissociating into its bare constituents, with the electrically charged one propagating (invariantly with a Feynman propagator) until the instant when it is scattered onto its mass shell by the incident virtual photon. The final state re-scatterings between the bare constituents will be shown to vanish in the scaling limit so that the constituents may be regarded as being scattered independently of one another, just as in the usual impulse approximation. Furthermore, for the physical proton in which the charged constituent is a bare proton of spin $\frac{1}{2}$ so that $m_p W_1 = \frac{1}{2x} [vW_2]$, we find that as $x \rightarrow 1$ both the W_1 and vW_2 functions approach zero as $(1-x)^3$ where x is the customary scaling variable. This is rather encouraging, since it is in good agreement with the present experimental result, unlike most spin $\frac{1}{2}$ parton models¹¹ with an ad hoc transverse momentum cut-off which lead naturally to a linear $(1-x)$ dependence as $x \rightarrow 1$.

The same bound-state wave function can also be used to evaluate the electromagnetic form factors F_1 and F_2 of a physical nucleon. Both these form factors depend on the square of the wave function ϕ . It can be readily shown that, on account of (1.3), as the square of the 4-momentum transfer $q^2 \rightarrow \infty$, apart from factors of

In q^2 , both F_1 and F_2 are $O(q^{-4})$, in agreement with the theoretical conclusion previously reached by others¹⁰, and with the threshold rule¹² relating the power of $(1-x)$ in the W_1 function and the power of the q^2 -dependence in the elastic form factors. This result has its parallel in the treatment of the non-relativistic bound-state problem with the Schrödinger equation. Equation (1.3) is the Bethe-Salpeter analogue of the condition that the wave function and hence the charge density is finite at the origin, from which it also follows that the form factor F_1 is $O(q^{-4})$ as $q \rightarrow \infty$.

In section II, we also discuss the forward Compton scattering amplitude and prove an Adler sum rule, which provides a convenient normalization condition for the bound-state solution of the Bethe-Salpeter equation. In addition, the crossing property to the annihilation channel $e + \bar{e} \rightarrow \bar{p} + \text{anything}$ is discussed in the same section.

While the Bethe-Salpeter equation is useful in illustrating the relation between the scaling property and the bound state system in a relativistic field theory, it has some obvious limitations for practical applications. Apart from the mathematical complexity of solving the Bethe-Salpeter equation, the covariant potential $V(q)$ is not known, the ladder approximation is not to be trusted, and furthermore, one cannot expect a simple two-particle bound state description of the physical nucleon to be an adequate one; due to virtual meson exchanges, there must be some additional multi-particle components present. Thus, for further insight as well as for practical applications, we adopt in section III a phenomenological approach by assuming that, instead, the bound-state wave function ϕ is known. The W_1 and νW_2 functions can then be directly evaluated in terms of a phenomenological set of diagrams which are based on the usual set of Feynman diagrams for the bound state. In particular, the implications of the physical picture of a proton as a bound state on the singularity structure

and asymptotic behavior of these diagrams are explored. This phenomenological description also allows us to generalize the two-particle bound state concept to include some multi-particle components, which in turn makes it possible for a more detailed comparison between the present experimental results and some simple model calculations.

In section IV, a simple ansatz for the multi-particle final state is made and the results of this model for deep inelastic electron scattering processes are given. In section V we first consider some further applications of the model, such as the polarization effect, then discuss some open questions, including "Where are these bare constituents to be found in nature?", "What might be the final meson multiplicity?" and "Is scaling an exact law in the infinite energy limit?", and finally we compare our approach to some related work of others.

II. Bethe-Salpeter Equation

In this section we shall discuss some general properties of the bound-state solution of a Bethe-Salpeter equation in the ladder approximation^{10,13}. For definiteness, we assume the bound-state solution to represent the physical proton p , and that it is composed of a spin $\frac{1}{2}$ particle P (the bare proton) of mass M and a spin 0 particle X^0 (the bare meson) of mass μ . It is convenient to use p_v , P_v and X_v to denote, respectively, the 4-momenta of the particles p , P and X^0 . Therefore, one has

$$p_v = P_v + X_v. \quad (2.1)$$

A. Bound state wave function

The equation for the bound-state wave function $\phi_p(k)$ can be written as¹⁴

$$\phi_p(k) = i\lambda \int V(k-k') K_p^{-1}(k') \phi_p(k') d^4k' \quad (2.2)$$

where

$$K_p(k) \equiv (-i\gamma \cdot P - M + i\epsilon)(X^2 + \mu^2 - i\epsilon), \quad (2.3)$$

$\epsilon = 0+$, V is the covariant potential given by (1.1), λ is the coupling constant, k is the relative momentum given by the usual expression

$$k_v = (M + \mu)^{-1} (\mu P_v - M X_v), \quad (2.4)$$

the solution $\phi_p(k)$ is a 4-component Dirac spinor function and the subscript p indicates that the total 4-momentum p_λ acts as a constant parameter for the integral equation.

It is useful to introduce an associated wave function $\psi_p(k)$, defined by

$$\psi_p(k) \equiv K_p^{-1}(k) \phi_p(k), \quad (2.5)$$

which differs from $\phi_p(k)$ only in the inclusion of the free propagator $K_p^{-1}(k)$. In terms of $\psi_p(k)$, Eq. (2.2) becomes

$$\phi_p(k) = K_p(k) \psi_p(k) = i\lambda \int V(k-k') \psi_p(k') d^4k'. \quad (2.6)$$

Both the wave functions $\phi_p(k)$, $\psi_p(k)$ and the free propagator $K_p(k)$ depend implicitly on the total 4-momentum p_λ . For a given V , by setting

$$p^2 = -m_p^2, \quad (2.7)$$

Eq. (2.2), or (2.6), can be regarded as an eigenvalue equation for the coupling constant λ .

The asymptotic behavior of $\phi_p(k)$ at large k can be readily obtained from (2.6) by taking V outside the integral, provided that

$$\int \psi_p(k') d^4k' \text{ is finite.} \quad (2.8)$$

That this provision (2.8) is indeed a correct one will be established in Appendix A.

From (1.2), (2.6) and (2.8), it follows then¹⁵

$$\phi_p(k) \sim 0(k^{-2}) \quad \text{as } k^2 \rightarrow \pm \infty. \quad (2.9)$$

[In Appendix A, the next order correction term to this asymptotic behavior will also be given.] It is also a consequence of the provision (2.8) that in the coordinate space the bound state solution is regular at the origin. [See (A. 19) in Appendix A.] This

is the relativistic analogue of the familiar result for a non-relativistic two-particle system. The bound-state solution of the Schrödinger equation for two particles interacting via a static Yukawa potential is also finite at the origin.

B. Conjugate solution

In a collision process, if the bound-state system is present in the initial state, then one can simply use the solution $\phi_p(k)$. On the other hand, if the bound-state system is in the final state then one cannot simply use its Hermitian conjugate $\phi_p^\dagger(k)$. This is because in the bound-state solution, each of the constituents, either P or X , can separately be on its mass shell, and therefore the $i\epsilon$ term in (2.3) is of importance. To derive the correct conjugate solution, called $\bar{\phi}_p(k)$, appropriate for the final state description, we shall make use of the time-reversal operation.

It is convenient to first introduce a 4×4 matrix $\Gamma_p(k)$ which relates the bound-state wave function $\psi_p(k)$ to that of a free Dirac spinor u_p :

$$\psi_p(k) = \Gamma_p(k) u_p \quad (2.10)$$

where u_p satisfies the free Dirac equation

$$(-i \gamma \cdot p - m_p) u_p = 0 \quad (2.11)$$

The matrix $\Gamma_p(k)$ satisfies an equation identical to that of $\psi_p(k)$; i.e.,

$$K_p(k) \Gamma_p(k) = i\lambda \int V(k-k') \Gamma_p(k') d^4k' \quad (2.12)$$

For definiteness, let us adopt the usual Pauli representation¹⁴ of the Dirac matrices.

Under the time-reversal operation, $\Gamma_p(k)$ becomes $[\Gamma_p(k)]_T$, which is related to the complex conjugate $\Gamma_p(k)^*$ by

$$\sigma_2 [\Gamma_p(k)]_T \sigma_2 = \Gamma_p(k)^* . \quad (2.13)$$

From (2.12) and assuming that V is real, one sees that the Hermitian conjugate of $[\Gamma_p(k)]_T$ satisfies

$$[\Gamma_p(k)]_T^\dagger K_p(k) = i \lambda \int [\Gamma_p(k')]_T^\dagger V(k - k') d^4 k' . \quad (2.14)$$

The conjugate solutions $\bar{\phi}_p(k)$ and $\bar{\psi}_p(k)$ are defined to be

$$\bar{\psi}_p(k) \equiv u_p^\dagger \gamma_4 [\Gamma_p(k)]_T^\dagger \quad (2.15)$$

and

$$\bar{\phi}_p(k) \equiv u_p^\dagger \gamma_4 [\Gamma_p(k)]_T^\dagger K_p(k) .$$

Equation (2.14) implies that these conjugate wave functions satisfy

$$\bar{\phi}_p(k) = \bar{\psi}_p(k) K_p(k) = i \lambda \int \bar{\psi}_p(k') V(k - k') d^4 k' . \quad (2.16)$$

In Figure 1, we give the standard graphical representation of the bound state wave function $\phi_p(k)$ and its conjugate solution $\bar{\phi}_p(k)$. It is important to note that these conjugate functions $\bar{\phi}_p(k)$ and $\bar{\psi}_p(k)$ are not the time-reversed solutions of $\phi_p(k)$ and $\psi_p(k)$; rather, their relation with $\phi_p(k)$ and $\psi_p(k)$ is the same as that between any outgoing wave and its corresponding incoming wave in a scattering process.

C. Normalization condition and some simple identities

In terms of the usual Feynman diagram given in Fig. 2, the matrix element of the electromagnetic current operator J_v between an initial physical proton state of 4-momentum p_v and a final physical proton state of 4-momentum

$$p'_v = p_v + q_v$$

can be readily derived. Since the electromagnetic vertex of a "bare" proton is simply $i e \gamma_v$, one finds for the physical proton

$$\langle p' | J_v | p \rangle = -e (2\pi)^{-4} \int d^4k (X^2 + \mu^2) \bar{\psi}_p(k') \gamma_v \psi_p(k) \quad (2.17)$$

where X_v is related to p_v and k_v through (2.1) and (2.4), and k'_v denotes the relative momentum in the final state which is given by

$$k'_v = k_v + (M + \mu)^{-1} \mu q_v \quad (2.18)$$

Since the physical proton has unit charge e , one must have

$$\langle p' | J_v | p \rangle \rightarrow e (p_v / m_p) \quad \text{as } q_v \rightarrow 0 \quad (2.19)$$

Therefore, the wave function $\psi_p(k)$ satisfies the normalization condition

$$(2\pi)^{-4} \int d^4k (X^2 + \mu^2) \bar{\psi}_p(k) \gamma_v \psi_p(k) = - (p_v / m_p) \quad (2.20)$$

In addition, $\psi_p(k)$, or $\phi_p(k)$, satisfies some simple identities which are listed below:

$$(i) \quad \int_p \bar{\psi}_p(k) \left[\frac{\partial K_p(k)}{\partial k_v} \right] \psi_p(k) d^4k = 0 \quad (2.21)$$

or

$$\int \bar{\phi}_p(k) \left[\frac{\partial K_p^{-1}(k)}{\partial k_v} \right]_p \phi_p(k) d^4k = 0$$

where the subscript p outside the square bracket indicates that the total 4-momentum p_v is kept fixed in the differentiation.

(ii) The normalization condition (2.20) can also be written as

$$i (2\pi)^{-4} \int \bar{\psi}_p(k) K_p(k) \psi_p(k) d^4k = [d \ln \lambda / d m_p]^{-1} . \quad (2.22)$$

The proofs of these identities are elementary; for completeness, they are given in Appendix B.

So far as the bound-state equation (2.6) is concerned, the charge of the constituents is irrelevant. Thus, the solution $\psi_p(k)$, or $\phi_p(k)$, can be applied equally well to the case in which the physical proton p is composed of, say, a bare neutron N and a bare π^+ (replacing P and X^0 , respectively). Instead of the spin $\frac{1}{2}$ constituent, it is now the spin 0 constituent that has a non-zero electromagnetic vertex. The first identity (2.21) insures that the limiting behavior (2.19) remains correct, as it should be. Or, one may also regard the bound-state solution $\psi_p(k)$, or $\phi_p(k)$, as describing a physical neutron n composed of a bare proton P and a bare π^- . The same identity (2.21) insures that for the physical neutron state

$$\langle n' | J_v | n \rangle \rightarrow 0 \quad \text{as } q_v = (n' - n)_v \rightarrow 0 . \quad (2.23)$$

Of course, if the physical neutron were composed only of an X^0 and a bare neutron N , then $\langle n' | J_v | n \rangle$ would be zero identically. The second identity (2.22) makes

it possible to express the normalization condition (2.20) in terms of a single loop diagram without the electromagnetic vertex¹⁶, as illustrated in Figure 2.

As we shall see in the following section G, the normalization condition (2.20) can be written in still another equivalent form which is related to Adler's sum rule¹⁷.

D. Electromagnetic form factor

To obtain the asymptotic behavior of the electromagnetic form factor for a physical proton state, it is most convenient to express $\langle p' | J_\nu | p \rangle$ in terms of $\phi_p(k)$. Equation (2.17) can be written as

$$\begin{aligned} \langle p' | J_\nu | p \rangle &= -e (2\pi)^{-4} \int d^4X (X^2 + \mu^2)^{-1} \bar{\phi}_p(k') (-i \gamma \cdot P' - M)^{-1} \gamma_\nu \\ &\quad \cdot (-i \gamma \cdot P - M)^{-1} \phi_p(k) \end{aligned} \quad (2.24)$$

where p_ν , k_ν , P_ν and X_ν are related by (2.1) and (2.4), $P'_\nu = P_\nu + q_\nu$, and therefore

$$p'_\nu = P'_\nu + X_\nu \quad (2.25)$$

and

$$k'_\nu = (M + \mu)^{-1} (\mu P'_\nu - M X_\nu) .$$

It can be readily verified by using (2.6) and (2.16) that the current conservation law holds; i.e.,

$$q_\nu \langle p' | J_\nu | p \rangle = 0 . \quad (2.26)$$

Thus, one may write

$$\langle p' | J_\nu | p \rangle = i e u_{p'}^\dagger \gamma_4 \left[\gamma_\nu F_1(q^2) + (2m_p)^{-1} \kappa q_\mu \sigma_{\mu\nu} F_2(q^2) \right] u_p \quad (2.27)$$

where u_p and $u_{p'}$ are, respectively, the free Dirac spinors with 4-momenta p_v and p'_v , $\sigma_{\mu\nu} = (2i)^{-1}(\gamma_\mu \gamma_\nu - \gamma_\nu \gamma_\mu)$, κ is the anomalous magnetic moment and $F_1(q^2)$, $F_2(q^2)$ are the usual charge and Pauli form factors.

We observe that in the integral (2.24) as $q^2 \rightarrow \infty$, if, say, in the laboratory frame the integration variable X_v is finite, then $P_v = p_v - X_v$ and $k_v = (M + \mu)^{-1} \mu p_v - X_v$ remain finite, but $(-i\gamma \cdot P' - M)^{-1} \phi_p(k')$ is $O(q^{-3})$, on account of (2.9); therefore, the integration over finite regions of X_v contributes $O(q^{-4})$ to both $F_1(q^2)$ and $F_2(q^2)$, apart from possible factors of $\ln q^2$. If the integration variable X_v itself is $O(q)$, then the entire integrand in (2.24) is $O(q^{-8})$ but d^4X is $O(q^4)$; therefore, the integration over the $X_v = O(q)$ region gives also a $O(q^{-4})$ contribution to $F_1(q^2)$, though a $O(q^{-6})$ contribution to $F_2(q^2)$.

To ascertain the $\ln q^2$ factor, we may assume for large k^2 , that $\phi_p(k)$ is proportional to $(k^2 + \lambda^2)^{-1}$. A direct calculation then leads to¹⁰

$$F_1(q^2) = O \left[\frac{1}{q^4} (\ln q^2)^2 \right]$$

(2.28)

and

$$F_2(q^2) = O \left[\frac{1}{q^4} \right].$$

This is in qualitative accord with present data according to which for $q^2 \lesssim 25 \text{ GeV}^2$

$$G_M(q^2) \equiv F_1 + \kappa F_2 \propto (q^2 + m^2)^{-2}$$

where $m^2 \cong 0.71 \text{ GeV}^2$. The electric form factor $G_E(q^2)$ is known¹⁸ only for $q^2 < 4 \text{ GeV}^2$, in which region it is proportional to $G_M(q^2)$:

$$(1 + \kappa) G_E(q^2) \approx G_M(q^2). \quad (2.29)$$

Since, by definition, $G_E(q^2) \equiv F_1 - (q^2/4M^2) \kappa F_2$ the model we are using predicts a deviation from the relation (2.29). Equation (2.28) may be wrong in detail, based as it is on so crude a model of the proton built of two bare constituents. However, as we shall see in the following, the physical model of a bound-state proton has led to the important general connection of the observed scaling in deep inelastic scattering with the rapid decrease of the electromagnetic form factors. We have shown here that a rapidly decreasing electromagnetic form factor, $F(q^2) \sim O(q^{-4})$ is implied for a bound-state solution of the Bethe-Salpeter equation that is regular at the origin. There is a parallel to this result in the non-relativistic Schrödinger theory for which the form factor of a bound state that is regular at the origin is also known to decrease at least as fast as $|\underline{q}|^{-4}$ where \underline{q} is the 3-momentum transfer¹⁹.

E. Structure functions

Next, we discuss the inelastic ep scattering

$$e + p \rightarrow p + X^0. \quad (2.30)$$

In the simple model of a two-body bound state where the covariant potential V is regarded phenomenologically as a given non-local function, this is the only reaction for the deep inelastic ep scattering process. There are two Feynman diagrams, labeled I_V and I'_V in Figure 3. One finds that (in the usual Feynman gauge)

$$I_V = e u_p^\dagger \gamma_4 \gamma_V [-i \gamma \cdot (P-q) - M]^{-1} \phi_p(k_{in}) \quad (2.31)$$

and

$$I'_V = ie (2\pi)^{-4} \int u_p^\dagger \gamma_4 \langle k_f | T_{p+q} | k' \rangle [-i \gamma \cdot P' - M]^{-1} \\ \cdot \gamma_V [-i \gamma \cdot (p - X') - M]^{-1} [X'^2 + \mu^2]^{-1} \phi_p(k_{in}) d^4 X' \quad (2.32)$$

where q_v is the virtual photon momentum, k_{in} and k_f denote, respectively, the relative momenta between the P and X^0 in the initial bound state and in the final continuum state, u_p denotes a free Dirac spinor of 4-momentum P_v , and the matrix T is the two-body scattering matrix defined by

$$\langle k | T_{p+q} | k' \rangle = i\lambda V(k' - k) + (i\lambda)^2 (2\pi)^{-4} \int d^4 k'' V(k' - k'') K_{p+q}(k'') V(k'' - k) + \dots \quad (2.33)$$

in which the subscript $p + q$ denotes the total 4-momentum of the system, k' and k are, respectively, the initial and final relative momenta for the two-body scattering process.

The diagram I_v , by itself, is not gauge invariant. As can be readily checked from the three preceding equations, the sum $I_v + I'_v$, of course, does satisfy

$$q_v (I_v + I'_v) = 0.$$

It is useful to decompose the amplitude I_v into a sum of a longitudinal part $(I_{\parallel})_v$ and a transverse part $(I_{\perp})_v$, and similarly $I'_v = (I'_{\parallel})_v + (I'_{\perp})_v$ such that $q_v (I_{\perp})_v = q_v (I'_{\perp})_v = 0$. While the two longitudinal amplitudes $(I_{\parallel})_v$ and $(I'_{\parallel})_v$ are related through the gauge transformation, the two transverse ones are not. As we shall see, in the scaling limit only $(I_{\perp})_v$ is of importance.

We note that the diagram I_v is identical in form to a corresponding one in the usual perturbation series in a standard pseudoscalar-coupling meson theory, except that in its evaluation the usual free spinor is now being replaced by the bound-state wave function $\phi_p(k_{in})$. Since the usual perturbation diagram fails to scale only by a $\ln v$ factor, the presence of $\phi_p(k_{in})$ is sufficient to satisfy the scaling property for

the present case because of the asymptotic behavior (2.9). By using (2.9) and (2.31), one can readily verify that in the scaling limit the diagram I_v gives a finite and non-zero contribution to the transverse structure function W_1 , but a zero contribution to the longitudinal structure function W_L which is related to the standard W_1 and νW_2 functions^{1,2} by

$$\nu W_2 = 2 \times m_p (W_1 + W_L) . \quad (2.34)$$

To derive the contribution of the diagram I'_v , it is most convenient to use, say, the laboratory frame. The essential point is the observation that the behavior of I'_v is determined by the configuration in which the virtual momentum P' of the bare proton is $0(q_v)$. Since each of the loop integrations in the diagrams for $\langle k | T_{p+q} | k' \rangle$ is a convergent one and since the additional loop integration over X' in the diagram for I'_v is a superconvergent one, the integral (2.32) remains convergent if the bare proton propagator with the large momentum P' is taken outside the integral. [Actually, it remains convergent if, in addition, one takes out also the boson propagator.] It is then easy to verify that in the scaling limit, compared to $(I_\perp)_v$ the transverse part $(I'_\perp)_v$ is smaller by a factor $0(q^{-2})$, and consequently the diagram I'_v does not contribute to W_1 . Furthermore, its longitudinal part $(I'_\parallel)_v$, like $(I_\parallel)_v$, makes zero contribution to W_L . The entire diagram I'_v can therefore be neglected in the scaling limit. For completeness, a detailed derivation of this result is presented in Appendix C.

With the vanishing of the re-scattering diagram I'_v in Figure 3 in the scaling region, we have now derived, in the context of this model, a fully relativistic generalization of the "parton" model. We find that the amplitude I_v gives an invariant

expression in (2.31) of the bare constituent, or parton, propagating invariantly and scattering independently onto its mass shell in the scaling region. [This replaces the usual parton theory amplitude of elastic scattering of an almost free parton in the impulse approximation.]

To derive the general functional form of the structure functions in the scaling limit, one needs only the value of the bound-state wave function $\phi_p(k)$ when one of its constituents, X^0 , is on its mass shell. Let us define

$$\lim_{X^2 + \mu^2 = 0} \phi_p(k) \equiv g(K) \gamma_5 u_p \quad (2.35)$$

where, for clarity, the 4-momenta of the two constituents X^0 and P in the bound state are labeled, respectively, by X_v and K_v . Thus, in diagram I_v given in Figure 3, one has

$$K_v = p_v - X_v = P_v - q_v. \quad (2.36)$$

On account of (2.9), the function g satisfies

$$g \sim 0(K^{-2}) \quad \text{as } K^2 \rightarrow \pm \infty. \quad (2.37)$$

Furthermore, as will be shown in Appendix A, in this limit $K^2 \rightarrow \pm \infty$, g is a c-number function independent of γ -matrices. By using (2.31) and (2.35), one finds that in the scaling limit

$$W_L \rightarrow 0, \quad (2.38)$$

$$W_1 \propto \int_{u_{\min}}^{+\infty} \frac{du}{(u + M^2)^2} |g(u)|^2 \left\{ (u + M^2)(1-x) + x [(M - m_p)^2 - \mu^2] \right\} \quad (2.39)$$

with

$$u_{\min} = \frac{\mu^2 x}{1-x} - m_p^2 x$$

and $x = -(2p \cdot q)^{-1} q^2$ is the usual scaling variable. The variable $u = K^2 = (P - q)^2$, and u_{\min} is the minimum invariant momentum transfer carried by the bare proton in diagram I_v of Figure 3. In terms of u , (2.37) becomes

$$g(u) \sim 0(u^{-1}) \quad \text{as } u \rightarrow \pm \infty. \quad (2.40)$$

We note that, before the scaling limit, the upper limit u_{\max} of the integral in (2.39) would be $-2p \cdot q$; because of the above convergence property of the bound-state wave function $g(u)$, one may set u_{\max} to be ∞ in the scaling limit. Now, the lower limit u_{\min} grows as $(1-x)^{-1}$ as $x \rightarrow 1$; therefore, in the scaling limit, (2.39) shows explicitly that the wave function is being probed for large values of u , or at "small distances". Furthermore, by using (2.40) we find that

$$W_1 \sim 0[(1-x)^3] \quad \text{as } x \rightarrow 1. \quad (2.41)$$

This is in agreement with the threshold relation¹² since $F_1(q^2) \sim 0(q^{-4})$ in this model.

The important physical point is that detailed study of W_1 near $x = 1$ measures the bound-state wave function of the nucleon. For example, if $g(u)$ is $\sim 0(u^{-n})$ as $u \rightarrow \infty$, then, according to (2.39), W_1 would be $\sim 0[(1-x)^{1+2n}]$ as $x \rightarrow 1$.

This behavior is also in accord with the threshold relation; i.e., F_1 will be $0(q^{-2-2n})$ as $q^2 \rightarrow \infty$. To see this, repeat the arguments leading to (2.9), observing that we must replace the potential in (1.2) by $V(q) \sim 0(q^{-2n})$ in order to obtain the asymptotic behavior $\phi_p(k) \sim 0(k^{-2n})$ from (2.6). By repeating the identical arguments given above (2.28), the stated result can be proved.

In the present simple model where the physical proton consists of only a two-body bound state, one sees that, according to (2.39)

$$W_1 \rightarrow \text{constant} \quad \text{as } x \rightarrow 0 \quad (2.42)$$

and therefore

$$\nu W_2 = 2 x m_p W_1 \rightarrow 0 \quad \text{as } x \rightarrow 0 \quad (2.43)$$

In the hypothetical case that the "bare" proton is, like the X^0 , also of spin 0 and, in addition, the covariant potential $V(q)$ is simply q^{-2} , then the exact bound-state solution is known^{20, 21} and the corresponding $g(u)$ is given simply by

$$g(u) = \text{constant} \cdot (u + M^2)^{-1} \quad (2.44)$$

If in the present case of a spin $\frac{1}{2}$ bare proton, one makes the ad hoc assumption that $g(u)$ remains given by (2.44), then one finds

$$W_1 = \text{constant} \cdot \frac{(1-x)^3 \left\{ (1-x)(M^2 - m_p^2 x) + \frac{1}{3} x [2(M - m_p)^2 + \mu^2] \right\}}{[\mu^2 x + (M^2 - m_p^2 x)(1-x)]^3} \quad (2.45)$$

which, of course, satisfies both (2.41) and (2.42).

F. Forward Compton scattering

We now want to verify directly that the structure functions computed in this model are in fact the absorptive parts of the forward Compton scattering amplitude in the scaling region. That is precisely how W_1 and W_2 are defined in general; however, in calculating these structure functions in the preceding section we have

used only the inelastic reaction (2.30) while ignoring all other final states consisting of $(P + X^0 + \text{gluons})$ where the gluons refer to the quanta of whatever fields are responsible for generating the covariant Yukawa potential between the two constituents P and X^0 . Such on-mass-shell states contribute to the absorptive part of the forward Compton amplitude although they are not included in our calculation of the preceding section. Nevertheless it will be shown that in the scaling limit these additional states are not important in the framework of our Bethe-Salpeter model with the ladder approximation. (For further discussions, see the remark given at the end of this section and also comments D and E in section V.)

In the present simple two-body bound-state model the spin-averaged forward amplitude $F_{\lambda\nu}(p, q)$ for the Compton scattering

$$\gamma + p \rightarrow \gamma + p$$

of a virtual (or real) photon of 4-momentum q_ν on a physical proton of 4-momentum p_ν can be written as a sum of four terms

$$F_{\lambda\nu} = A_{\lambda\nu}(p, q) + A_{\nu\lambda}(p, -q) + B_{\lambda\nu}(p, q) + B_{\nu\lambda}(p, -q) \quad (2.46)$$

where $A_{\lambda\nu}(p, q)$ and $B_{\lambda\nu}(p, q)$ represent the corresponding diagrams in Figure 4, and $A_{\nu\lambda}(p, -q)$ and $B_{\nu\lambda}(p, -q)$ denote, respectively, the same diagrams but with the two external photons exchanged. The explicit expressions of $A_{\lambda\nu}$ and $B_{\lambda\nu}$ are given by

$$A_{\lambda\nu}(p, q) = i \int (2\pi)^{-4} d^4X (X^2 + \mu^2)^{-1} \bar{\phi}_p(k_{in}) [-i\gamma \cdot (p-X) - M]^{-1} \gamma_\nu [-i\gamma \cdot p - M]^{-1} \\ \cdot \gamma_\lambda [-i\gamma \cdot (p-X) - M]^{-1} \phi_p(k_{in}) \quad , \quad (2.47)$$

$$\begin{aligned}
B_{\lambda\nu}(p, q) = & i \int (2\pi)^{-8} d^4X d^4X' (X^2 + \mu^2)^{-1} (X'^2 + \mu^2)^{-1} \bar{\phi}_p(k_f) [-i \gamma \cdot (p - X) - M]^{-1} \\
& \cdot \gamma_\nu [-i \gamma \cdot P - M]^{-1} \langle k | T_{p+q} | k' \rangle [-i \gamma \cdot P' - M]^{-1} \gamma_\lambda \\
& \cdot [-i \gamma \cdot (p - X') - M]^{-1} \phi_p(k_{in})
\end{aligned} \tag{2.48}$$

where X_ν and X'_ν are the 4-momenta of X^0 as labeled in Figure 4,

$$P = p + q - X, \quad P' = p + q - X', \tag{2.49}$$

k_{in} and k_f denote the appropriate relative momenta in the bound state, given respectively by

$$k_{in} = (M + \mu)^{-1} \mu p - X'$$

and

$$k_f = (M + \mu)^{-1} \mu p - X,$$

k and k' are the relative momenta in the continuum states, related to X , P and X' , P' by

$$k = (M + \mu)^{-1} (\mu P - MX)$$

and

$$k' = (M + \mu)^{-1} (\mu P' - MX'),$$

and $\langle k | T_{p+q} | k' \rangle$ is given by (2.33). By using the Bethe-Salpeter equation (2.2), one can readily verify that $F_{\lambda\nu}$ satisfies the requirement of current conservation

$$q_\lambda F_{\lambda\nu} = 0. \tag{2.50}$$

Thus, $F_{\lambda\nu}$ can be written as

$$F_{\lambda\nu} = \left(\delta_{\lambda\nu} - \frac{q_\lambda q_\nu}{q^2} \right) U_1 + \frac{1}{m_p^2} \left(p_\lambda - \frac{p \cdot q}{q^2} q_\lambda \right) \left(p_\nu - \frac{p \cdot q}{q^2} q_\nu \right) U_2 \quad (2.51)$$

where U_1 and U_2 are scalar functions of q^2 and $\nu \equiv -m_p^{-1}(p \cdot q)$. In this section, we are only interested in the case of a space-like photon $q^2 > 0$ with $\nu > 0$.

As we have already noted, in the present model the absorptive parts (i.e., the imaginary parts) of U_1 and U_2 are, in general, different from the corresponding structure functions πW_1 and πW_2 calculated by using only the inelastic reaction (2.30). However, as we shall prove in Appendix D, in the limit $q^2 \rightarrow \infty$, $\nu \rightarrow \infty$, but keeping $x = (2m_p \nu)^{-1} q^2$ fixed,

$$\text{Im } U_1 \rightarrow \pi W_1$$

and

$$\text{Im } (\nu U_2) \rightarrow \pi (\nu W_2) \quad (2.52)$$

where W_1 is the same function given by (2.39) and $\nu W_2 = 2 \times m_p W_1$. Of course, had one included all diagrams, then $\text{Im } U_1 = \pi W_1$ and $\text{Im } U_2 = \pi W_2$ should hold at all values of q^2 and ν . The above expression (2.52) shows that under the ladder approximation these equalities are at least maintained in the scaling limit.

As will be shown in Appendix D, the diagram $B_{\lambda\nu}$ in Figure 4 can be neglected in the scaling limit. We emphasize that in the Bethe-Salpeter model with the ladder approximation, the gluons are exchanged only between different bare constituents. This is why in diagram $B_{\lambda\nu}$ these on-mass-shell intermediate $(P + X^0 + \text{gluons})$ states

are of no importance in the scaling limit. In a bona fide relativistic local field theory, there must be other forward Compton diagrams which contain gluon radiative corrections, or renormalizations; in these diagrams, there are emissions and absorptions of gluons by the same bare constituent. The imaginary part of these diagrams would correspond to gluon radiation in deep inelastic ep scattering; such processes lie outside the present framework of a simple two-body bound-state model, and are therefore not included in our calculations on structure functions. As will be discussed in comment E of section V, at least in a perturbation series, these additional gluon-radiation diagrams would lead to violations of the scaling property.

We note that, like the diagram I'_V in the previous section, the diagram $B_{\lambda V}$ contains an s -channel pole at $(p+q)^2 + m_p^2 = 0$. Both diagrams are needed for maintaining gauge invariance, and both can be neglected in the scaling limit.

G. Adler sum rule

In this section, we shall show that the normalization condition (2.20) implies that in the scaling limit the νW_2 function should satisfy

$$\int_0^1 x^{-1} dx (\nu W_2) = 1 \quad (2.53)$$

where $\nu W_2 = 2 \times m_p W_1$ and W_1 is given by (2.39). Equation (2.53) is (essentially) the Adler sum rule¹⁷, but applied to the present simple two-body bound-state model of the physical nucleon. By using (2.39), one sees that the above integral is a convergent one. Equation (2.53) then determines the proportionality constant in (2.39). Our interest in deriving (2.53), or equivalently in our model, in proving the Adler sum rule stems from the fact that, on the basis of (2.20) alone we cannot in practice normalize

our structure functions. This is because we have not solved the Bethe-Salpeter equation explicitly for the wave function; we have simply derived those general properties and the asymptotic behavior of $\psi_p(k)$ as required to establish scaling properties, asymptotic behaviors of the elastic form factors, and the threshold theorems. In normalizing the current in (2.20) we have to know the exact wave function $\psi_p(k)$ for all momenta k_μ which is integrated over its entire range, while in evaluating vW_2 we need only $g(u)$, which is, according to (2.35), determined by $\psi_p(k)$ when one of the constituents, X^0 , is on its mass shell. The sum rule (2.53) provides the needed normalization of the structure functions for our purposes.

It is useful to define a new scattering amplitude

$$F'_{\lambda\nu}(p, q) \equiv A_{\lambda\nu}(p, q) - A_{\nu\lambda}(p, -q) + B_{\lambda\nu}(p, q) - B_{\nu\lambda}(p, -q) \quad (2.54)$$

where $A_{\lambda\nu}$ and $B_{\lambda\nu}$ are given respectively by (2.47) and (2.48). If one wishes, one may relate $F'_{\lambda\nu}$ to the vector part of the $\bar{v}p$ scattering amplitude. However, for the purpose of deriving (2.53), the precise nature of the physical process that is represented by this amplitude $F'_{\lambda\nu}$ is immaterial. By definition, $F'_{\lambda\nu}$ satisfies

$$F'_{\lambda\nu}(p, q) = -F'_{\nu\lambda}(p, -q) . \quad (2.55)$$

By using the Bethe-Salpeter equation (2.2) and the normalization condition (2.20), one can readily establish the divergence condition

$$q_\nu F'_{\lambda\nu} = 2m_p^{-1} p_\lambda \quad (2.56)$$

and therefore

$$q_\lambda q_\nu F'_{\lambda\nu} = 2m_p^{-1} (p \cdot q) = -2v . \quad (2.57)$$

Equation (2.56) is the crucial result, since it plays the role of current algebra in the usual derivation. Once we have established the divergence condition, we need only verify that $F'_{\lambda\nu}$ satisfies appropriate convergence requirements (unsubtracted dispersion relations) when $\nu \rightarrow \infty$. This is explicitly clear in the discussions of Adler and Bjorken¹⁷. We reproduce the necessary algebra in Appendix E, commenting here only that the asymptotic behavior of the wave function (1.3) insures the required convergence properties which establish (2.53). In the literature, the Adler sum rule has been derived for the part of the forward Compton amplitude that is odd under crossing, that is for the difference of amplitudes for neutrinos and antineutrinos incident on a given target nucleon. In our model with a single charged nucleon in the bound state, the coupling of the z-component isospin I_3 (electromagnetic) current to the proton is just $2^{-\frac{1}{2}}$ in strength relative to that of the usual $I_{\pm} = 2^{-\frac{1}{2}}(I_1 \pm i I_2)$ current in the weak interaction.

H. Crossing to the annihilation channel

The physical process of

$$e + \bar{e} \rightarrow \bar{p} + \text{anything} \quad (2.58 a)$$

is related to deep inelastic scattering

$$e + p \rightarrow e + \text{anything} \quad (2.58 b)$$

by crossing symmetry. In a perturbation calculation of these processes, this can be proved by applying the usual substitution rule to each Feynman graph order by order.

It has been shown⁶ that this symmetry persists in the cut-off field theory model and that

as a consequence the structure functions for (2.58a), (\bar{W}_1, \bar{W}_2) , are analytic continuations into the physical region for this process of the structure functions for (2.58b), (W_1, W_2) . Moreover, the scaling behavior for these functions has been derived for the deep inelastic annihilation and scattering regions, respectively. In particular

$$\bar{W}_1(x) = W_1(x)$$

and

(2.59)

$$v\bar{W}_2(x) = vW_2(x) ;$$

i.e., \bar{W}_1 is the continuation of $W_1(x)$ from the physical region for (2.58b) with $x > 1$ to the physical region for (2.58a) with $x < 1$, where now $1/x$ is the fraction of the total $e\bar{e}$ collision energy deposited on the observed hadron in the collision center-of-mass system.

The practical value of (2.59) is its prediction of the magnitude of the cross section for (2.58a) near $x = 1$ in terms of scattering measurements. More generally, if we can prove (2.59) for our physical bound-state model, then we have a prediction of the threshold behavior for the inclusive annihilation process in accord with (2.41).

The crossing properties of the scattering amplitude depend on those of the wave function $g(u)$ appearing in it. Generally, we destroy crossing symmetry when working with the Bethe-Salpeter equation in the ladder approximation. However, for study of the threshold behavior we require only the solution for $g(u)$ for large values of u according to (2.40). For the inelastic scattering near threshold as $1 - x \rightarrow 0+$, $u \rightarrow +\infty$, whereas for the crossed or annihilation process the virtual intermediate constituent is timelike or masslike in Figure 4 with $u \rightarrow -\infty$. In both cases, (2.40)

states that $g(u) \sim 0 (u^{-1})$ as $u \rightarrow \pm \infty$. Therefore, (2.59) is valid near $x \sim 1$ for our bound state model. However, we have not studied the general crossing properties for arbitrary x .

III. Phenomenological Approach

In this section we reconstruct the results of the Bethe-Salpeter model of the preceding section by developing a phenomenological approach for studying a bound-state model of the proton's structure. Our starting point is the diagram I_V in Figure 3 and its corresponding amplitude, by (2.31) and (2.35):

$$I_V = e u_p^\dagger \gamma_4 \chi_V [-i \gamma \cdot (P-q) - M]^{-1} \gamma_5 u_p g(u) \quad (3.1)$$

where $g(u)$ is the wave function at the (pPX_0) vertex and is a function of the mass of the virtual P with both the p and X^0 on their mass shells. In this phenomenological approach, we shall for simplicity assume $g(u)$ to be strictly a c-number function, whereas in our previous discussions on the Bethe-Salpeter equation $g(u)$ is a c-number function only in the limit $u \rightarrow \infty$.

A. Current conservation

Equation (3.1) is not gauge invariant as noted earlier, and its completion requires that final state rescattering effects be added. Thus, in the Bethe-Salpeter approach we accomplish this by adding the diagrams I'_V in Figure 3. These take into account the fact that the exchange of quanta between the constituents P and X^0 that gave rise to the initial bound state of the physical proton is still occurring after the virtual photon q is absorbed. In the well known way, all possible insertions of the photon must be made on the charged line in Figure 3 in order to insure current conservation.

In constructing the terms which must be added to (3.1) in order to give us an overall current-conserving amplitude for inelastic scattering, we are guided by two

principles: the first is simplicity, and the second is our insistence not to introduce any "unwanted, unphysical" singularities in the amplitude. We may directly write in accord with these principles

$$II_v = +ie u_p^\dagger \gamma_4 \gamma_5 u_p \frac{(2p_v + q_v)}{[(p+q)^2 + m_p^2]} g(u) \quad (3.2)$$

so that $q_v(I_v + II_v) = 0$. This form has an s-channel pole at the bound-state proton mass, as it should. In the simple phenomenological approach, it seems sensible to choose only functions with simple poles. This is to be contrasted with our previous Bethe-Salpeter approach in which II_v is replaced by I_v' of (2.32) which has in addition to the same bound-state s-channel pole also cuts due to the continuum states. Of course, Eq. (3.2) is not unique and one can readily construct a more general term that, for simplicity, still retains the spin structure of (3.2) by writing

$$\tilde{II}_v = ie u_p^\dagger \gamma_4 \gamma_5 u_p [\lambda_1 p_v + \lambda_2 q_v + \lambda_3 P_v] \quad (3.3)$$

where λ_i are scalar functions of the three independent scalars

$$s \equiv (p+q)^2 ; \quad u \equiv (P-q)^2 ; \quad t \equiv (p-P)^2 ,$$

with

$$s + t + u = -[m_p^2 + M^2 + \mu^2 - q^2] . \quad (3.4)$$

Current conservation requires that the functions λ_i satisfy the restriction

$$\lambda_1 q \cdot p + \lambda_2 q^2 + \lambda_3 q \cdot P = g(u) . \quad (3.5)$$

Such a relation has no unique solution; we can add to any particular solution of (3.5)

arbitrary amounts, $\delta\lambda_1$, such that

$$\delta\lambda_1 q \cdot p + \delta\lambda_2 q^2 + \delta\lambda_3 q \cdot P = 0 . \quad (3.6)$$

This is equivalent to the observation that the restriction of current conservation fixes the amperian current interactions, but not the non-minimal terms proportional to electromagnetic field strengths and their derivatives. These are automatically gauge invariant. In our model we rule out all such non-minimal terms. For example, their presence in the interaction Lagrangian of a relativistic field theory calculation generally leads to non-renormalizable theories. If included in the electromagnetic interaction of the constituents (or partons), they violate scaling.

Returning to (3.5), we look for that solution which introduces no additional u -channel singularities since these are already contained in (3.1), i.e. the graph I_v in Figure 3. We also rule out t -channel singularities, or by (3.4), poles in the photon mass q^2 , since the X^0 is taken to be neutral with no direct electromagnetic interaction. We find therefore that (3.5) gives

$$\lambda_1 = 2\lambda_2 = \frac{2g(u)}{[(p+q)^2 + m_p^2]} ; \quad \lambda_3 = 0 \quad (3.7)$$

and (3.3) reduces to (3.2). We have now the inelastic scattering amplitude according to our criteria of simplicity, of minimal electromagnetic couplings, and of no unwanted singularities in the u - or t -channels.

B. Bound-state vs. elementary particle model of the proton

The difference between a physical model of the proton as a bound state of two constituents, and an elementary particle picture of the proton lies in the behavior of

the wave function $g(u)$. As we have already shown for a particular bound-state model in the ladder approximation to the Bethe-Salpeter equation, as illustrated in Figure 3, the wave function behaves as in (2.40); i. e.

$$g(u) \sim 0\left(\frac{1}{u}\right) \quad \text{for } u \rightarrow \pm \infty \quad (3.8)$$

where u is the virtual mass of either of the constituents forming the bound state. On the other hand, if the nucleon is elementary and there is an elementary vertex interaction, as illustrated in Figure 6, in place of $g(u) \gamma_5$ one has the vertex function $G \gamma_5$ where G is a constant in the lowest order perturbation calculation. Furthermore, even if one includes final state interactions with a potential given by (1.1), the effective vertex function G for the three-point function $p \rightarrow p + X^0$, after summing over all ladder diagrams in the final state of $p X^0$, remains dominated by this non-vanishing lowest order diagram at least at large u ; therefore, in the ladder approximation

$$G \rightarrow \text{constant for large } u. \quad (3.9)$$

This contrast between bound-state and elementary-particle descriptions of the nucleon has been analyzed and discussed in some detail by Ball and Zachariasen¹⁰.

From the view of the elementary-particle model, one may, of course, invoke the possibility that the final state strong interaction can be quite complicated, and that for some unknown reason the three-point vertex for $p \rightarrow p + X^0$ is given phenomenologically by $G \gamma_5$ where G does not satisfy (3.9); instead, it can be of a general form

$$G = G(p^2, P^2, X^2) \quad (3.10)$$

where p and P denote the initial and final momenta of the same elementary particle p , and X that of the boson as before. Because of crossing symmetry,

$$G(p^2, P^2, X^2) = G(P^2, p^2, X^2) .$$

As we shall see, even then there is an important difference between the elementary-particle approach and the bound-state approach.

As shown in Figure 6, there are at least two standard diagrams $\bar{\Gamma}_\lambda$ and $\bar{\Pi}_\lambda$ for the process

$$\gamma + p \rightarrow p + X^0$$

in the elementary particle approach. In these two diagrams, the electromagnetic vertex is assumed to be given by the usual minimal interaction $e \gamma_\lambda$. If G is a constant, or if G satisfies (3.9), then the result does not scale as noted before. With G given by (3.10), the sum of the first two amplitudes in Figure 6 is just

$$\begin{aligned} \bar{\Gamma}_\lambda + \bar{\Pi}_\lambda = & i e u_{p'}^\dagger \left[\gamma_5 \frac{1}{-i \gamma \cdot (p+q) - m} \gamma_\lambda G(s, -m^2, -\mu^2) \right. \\ & \left. + \gamma_\lambda \frac{1}{-i \gamma \cdot (p' - q) - m} \gamma_5 G(-m^2, u, -\mu^2) \right] u_p \end{aligned} \quad (3.11)$$

where m is the nucleon mass, q is the photon momentum, and p and p' denote respectively the initial and final proton momenta. If G is not a constant, then (3.11) has the defect of failing to conserve electromagnetic current, viz.

$$q_\lambda (\bar{\Gamma}_\lambda + \bar{\Pi}_\lambda) = -e u_{p'}^\dagger \gamma_4 \gamma_5 u_p \left\{ G(s, -m^2, -\mu^2) - G(-m^2, u, -\mu^2) \right\} . \quad (3.12)$$

One is led to remedy this defect in the usual manner by adding to the amplitude (3.11) a four-point contact interaction as the diagram $\overline{\text{III}}_\lambda$ in Figure 6 which is suitably tailored so that the additional contribution, $\overline{\text{III}}_\lambda$, restores current conservation to the overall amplitude:

$$q_\lambda (\overline{\text{I}}_\lambda + \overline{\text{II}}_\lambda + \overline{\text{III}}_\lambda) = 0 \quad . \quad (3.13)$$

As in our prior discussion of (3.3) and (3.4), there is no unique solution to this condition, but one usually searches for a "guess" that is both simple and free of unwanted singularities. In this elementary nucleon example, the latter condition means in particular that $\overline{\text{III}}_\lambda$ should contain neither s- nor u-channel poles since the direct and exchanged nucleon poles are already included in the two terms of (3.11). In contrast, for a bound-state physical model an s-channel pole was introduced in the gauge term in (3.2), since it represented the entire s-channel contribution. As we shall see, in the bound-state approach it is the presence of this growing denominator factor at high energies, $s \rightarrow \infty$, that leads to the limiting behavior that the gauge term vanishes in the scaling region. Without the large denominator, the gauge terms generally will grow and eventually destroy scaling behavior, as would be the case in the elementary-particle approach. For example, we may choose

$$\begin{aligned} \overline{\text{III}}_\lambda = & e u_p^\dagger \gamma_4 \gamma_5 u_p \left[\frac{G(s, -m^2, -\mu^2) - G(-m^2, -m^2, -\mu^2)}{s + m^2} (2p + q)_\lambda \right. \\ & \left. - \frac{G(-m^2, u, -\mu^2) - G(-m^2, -m^2, -\mu^2)}{u + m^2} (2p' - q)_\lambda \right] \end{aligned} \quad (3.14)$$

which satisfies (3.13), has no unwanted poles, and is also the result of the standard

minimal electromagnetic coupling; i.e., as can be readily verified, if one represents the three-point vertex $G \gamma_5$ by an effective Lagrangian, the formal replacement of $\frac{\partial}{\partial x_\lambda}$ by $\frac{\partial}{\partial x_\lambda} - ieA_\lambda$ for the charged field in the Lagrangian would lead to a four-point function given by (3.14). By choosing a sufficiently convergent function G , the contribution to the structure functions from the square of the first two amplitudes, $\bar{I}_\lambda + \bar{II}_\lambda$ in (3.13), can be easily made to vanish in the scaling limit. However, the third amplitude \bar{III}_λ survives in the scaling limit due to the constant vertex $G(-m^2, -m^2, -\mu^2)$ that was added to both terms to remove the s - and u -channel poles and leads to a logarithmic violation of scaling for the transverse function W_1 and a linear one for the longitudinal function W_L , and therefore also for νW_2 :

$$\nu W_2 \sim 0(\nu)$$

and

$$W_1 \rightarrow \text{constant} \int_{u_{\min}}^{2mv} \frac{u du}{(u+m^2)^2} G^2(-m^2, -m^2, -\mu^2) + \text{finite terms} \quad (3.15)$$

$$\propto \ln \frac{\nu}{m} + \dots$$

where $u_{\min} = \frac{\mu^2 x}{1-x} - m^2 x$. We can trace the origin of the difficulties leading to (3.15) to the appearance of an elementary s -channel pole term in the diagram \bar{II}_λ of Figure 6. No such diagram appears in the bound-state model because there is never a first moment for the electromagnetic current to interact with an elementary charged constituent "before" it finds itself bound into the physical proton. In the bound-state model, the s -channel pole term is introduced only through the final state interactions between the emerging constituents after they have been struck by the photon. In place of the amplitude $\bar{II}_\lambda + \bar{III}_\lambda$, one has the amplitude II_ν given by (3.2) in the simple phenomenological approach [or I'_ν , given by (2.32) in the Bethe-Salpeter approach].

For a bound-state proton with the wave function (3.8) it is easy to show that the contribution to the structure functions W_1 and νW_2 coming from the added "gauge" term, or Π_ν in (3.2), vanishes as $1/q^2$ in the scaling limit. This is because in the scaling region of large ν and q^2 the energy denominator in this amplitude is large, $\sim \nu$ or s , and cannot be cancelled by large numerator factors in integrating over the final two-particle phase space when the region of large u values is damped as in (3.8). Both the square of the gauge term Π_ν and its interference with I_ν can be computed for studying the approach to scaling, but the entire contribution in the scaling region comes only from the amplitude I_ν in (3.1). This conforms to the simple "parton" picture in that the relevant mechanism is the "dissociation" of a physical nucleon into its constituents as it interacts with the electromagnetic field. Whereas the parton model is limited to the infinite momentum frame, we have now a covariant and current-conserving description in terms of Feynman propagators. As expected, our final result in the phenomenological approach scales and coincides with (2.39), which was obtained previously in the Bethe-Salpeter approach.

We recall from section II that the same bound-state model of a proton that leads to a scaling behavior for the inelastic structure functions also predicts a rapid decrease of the electromagnetic form factors:

$$F_1(q^2) \sim 0 \left[\frac{1}{q^4} (\ln q^2)^2 \right] \text{ and } F_2(q^2) \sim 0 \left(\frac{1}{q} \right) \quad (3.16)$$

in qualitative accord with present data. Since the physical model constructed here with a phenomenological approach has the same wave function behavior for large momenta, i.e., $g(u) \sim 0 \left(\frac{1}{u} \right)$ for large u according to (3.8), we again find as in section II that

$W_1 \sim 0 [(1-x)^3]$ as $x \rightarrow 1$. As noted before, this is in agreement with the threshold relation by (3.16). Moreover, the crossing relation to the annihilation channel described in section II remains valid. Finally, we note that the added amplitude Π_V , as required for gauge invariance, can also lead to a sum rule (2.53) of the Adler type for normalizing the structure functions in the phenomenological approach.

While the simple phenomenological approach described in this section is guided by the Bethe-Salpeter equation, it has a greater heuristic value than our previous Bethe-Salpeter approach. It allows us to dissociate the rigid connection between the vertex function $g(u)$ and the solution of a particular class of equations based on the ladder approximation. For any given $g(u)$, the amplitude $(I_V + \Pi_V)$ is relativistically invariant and gauge invariant, thus allowing us to calculate directly the structure functions in the scaling limit as well as the approach to scaling.

IV. Simple Model Calculations

The description that a physical nucleon is only a two-body bound state is clearly an over-simplified one. Through virtual meson exchanges there also must be multi-meson channels connected to the physical nucleon state. Furthermore, as we shall see, the existence of such multi-meson channels can alter the limiting behavior of the structure functions as $x \rightarrow 0$; in particular, νW_2 may approach a constant, instead of zero as given by (2.43) for a two-body bound state.

A. First example

In order to illustrate such possibilities, we take as a first example a simple ansatz that the physical nucleon p or n consists of (i) a two-body state composed of a bare nucleon P or N and an SU_3 singlet X^0 , and (ii) a multi-body state composed of, at least, a bare SU_3 octet baryon and two SU_3 octet mesons, say $P \pi^0 \pi^0$, or $\Sigma^+ K^- \pi^+$, etc.; formally, one may write

$$p = (P X^0) + (P 2\pi) + (\Sigma K \pi) + \dots \quad (4.1)$$

etc. [The possibility that there should also be, in addition, a two-body $(P \pi)$ channel will be discussed later.] While the actual bound-state calculation for a multi-particle system is complicated, a phenomenological description, based on the bound-state idea, can be easily given. Following the discussion given in section III, we may represent the reaction

$$\gamma + p \rightarrow P + X^0 \quad (4.2)$$

by diagrams I_λ and II_λ in Figure 7, the reaction

$$\gamma + p \rightarrow P + \pi^0 + \pi^0 \quad (4.3)$$

by diagrams III_λ and IV_λ in the same Figure, etc. The amplitudes I_λ and II_λ are given by (3.1) and (3.2) respectively; i.e.

$$I_\lambda = e u_p^\dagger \gamma_4 \gamma_\lambda [-i \gamma \cdot (P - q) - M]^{-1} \gamma_5 u_p g \quad (4.4)$$

and

$$II_\lambda = ie u_p^\dagger \gamma_4 \gamma_5 u_p [(p + q)^2 + m_p^2]^{-1} (2p + q)_\lambda g \quad (4.5)$$

In complete analogy, the diagrams III_λ and IV_λ may be represented by

$$III_\lambda = ie u_p^\dagger \gamma_4 \gamma_\lambda [-i \gamma \cdot (P - q) - M]^{-1} u_p g' \quad (4.6)$$

and

$$IV_\lambda = -e u_p^\dagger \gamma_4 u_p [(p + q)^2 + m_p^2]^{-1} (2p + q)_\lambda g' \quad (4.7)$$

where, as before, g denotes the two-body bound-state wave function when X^0 is on the mass shell, and similarly g' denotes the three-body bound-state wave function when both mesons are on their mass shells. Thus, g depends only on one variable, say $u = (P - q)^2$, but g' depends on three variables, say $(p - \pi_a)^2$, $(p - \pi_b)^2$ and $u = (P - q)^2$ where π_a and π_b denote the final momenta of the two pions. It is easy to see that for arbitrary g and g' one has

$$q_\lambda (I_\lambda + II_\lambda) = 0$$

and

$$q_\lambda (III_\lambda + IV_\lambda) = 0 \quad (4.8)$$

In a phenomenological approach, g and g' may be assumed to be any reasonable wave functions. We note that according to (3.8)

$$g(u) \sim 0(u^{-1}) \quad \text{as } u \rightarrow \infty. \quad (4.9)$$

For definiteness, $g(u)$ may be assumed to be given by (2.44); i.e.,

$$g(u) \propto (u + M^2)^{-1} \quad (4.10)$$

which, we recall, is the rigorous solution of the Bethe-Salpeter equation if all particles are of zero spin and if $V(q^2)$ is q^{-2} . To assign a specific form to g' , there is at present very little theoretical guidance. Purely for reasons of computational simplicity, we choose as an ansatz for g'

$$g' = g'(u) \quad (4.11)$$

which depends only on u . Physically, this corresponds to the assumption that the 2π system behaves like a composite of a variable mass κ , and that as an extremely crude approximation g' is taken to be independent of the mass κ and the other internal variable of the 2π system. It is then straightforward to evaluate the structure function by using (4.6) and (4.7). We find that in the scaling limit, diagrams III_λ and IV_λ lead to a W_1 function given by

$$W_1 \propto \int_{4\mu^2}^{\infty} \sigma(\kappa) d\kappa^2 \int_{u_{\min}}^{\infty} \frac{du}{(u + M^2)^2} |g'(u)|^2 \left\{ (u + M^2)(1-x) + x [(M - m_p)^2 - \kappa^2] \right\} \quad (4.12)$$

where μ is the pion mass,

$$u_{\min} = \frac{\kappa^2 x}{1-x} - m_p^2 x \quad (4.13)$$

and $\sigma(\kappa)$ denotes the density of states for the 2π system which is given by

$$\sigma(\kappa) = \kappa^{-1} (\kappa^2 - 4\mu^2)^{\frac{1}{2}} . \quad (4.14)$$

As expected, the integrand inside the first integral in (4.12) is identical to that in (2.39) except for the replacement of g by g' and μ by κ .

From (4.12), one can readily verify that if

$$g'(u) \rightarrow 0(u^{-n}) \quad \text{as } u \rightarrow \infty \quad (4.15)$$

where $n \geq 1$, then

$$W_1 \rightarrow 0[(1-x)^{1+2n}] \quad \text{as } x \rightarrow 1 \quad (4.16)$$

and

$$W_1 \rightarrow 0(x^{-1}) \quad \text{as } x \rightarrow 0 . \quad (4.17)$$

This latter behavior is closely connected with the property that the density of states satisfies

$$\sigma(\kappa) \rightarrow \text{constant} \quad \text{as } \kappa \rightarrow \infty . \quad (4.18)$$

From a phenomenological point of view, the precise origin of the approximation (4.11) is not of immediate concern. We may regard (4.12) as representing the combined contributions of all multi-body states, not just the three-body state, provided that (4.11) and (4.18) serve as reasonable approximations.

To assign a specific value for n , we may be guided by the aforementioned crude physical picture of the $(P 2\pi)$ system. Let us neglect the $\pi-\pi$ interaction. The two pions, say π_a and π_b , are then bound only through the two-body πP potential V . The most elementary Feynman diagram for the three-body potential U

should consist of two bonds: one links π_a to P and the other π_b to P. Each bond gives a factor V, and therefore U is proportional to the square of V. Since as $q^2 \rightarrow \infty$, V is $\sim O(q^{-2})$, one may expect U to be $\sim O(q^{-4})$ where q denotes the 4-momentum transfer between P and the (2π) system, assuming that q is of the same order as the 4-momentum transfer between P and each individual pion. This crude picture suggests that as a pure trial form one may assume $n = 2$ in (4.15); i.e.

$$g' \sim O(u^{-2}) \quad \text{as } u \rightarrow \infty .$$

For definiteness of calculation, we make the further ad hoc assumptions that g is given by (4.10) with $M = m_p$, i.e., apart from normalization factors,

$$g = (u + m_p^2)^{-1} ,$$

and similarly g' is given by

$$g' = (u + m_p^2)^{-2} . \quad (4.19)$$

The result is then, for the physical proton

$$(W_1)_p = \beta_p [F_{II}(x) + \alpha_p F_I(x)] \quad (4.20)$$

where α_p and β_p are constants, the contribution due to the two-body channel is proportional to

$$F_I(x) = (1-x)^3 \frac{m_p^4 [m_p^2(1-x)^2 + \frac{1}{3} m_X^2 x]}{[m_p^2(1-x)^2 + m_X^2 x]^3} \quad (4.21)$$

and the contribution due to the multi-body channel is proportional to

$$F_{II}(x) = x^{-1} (1-x)^5 h(x) , \quad (4.22)$$

in which

$$h(x) = \frac{1}{64 (1-x)^6} \left\{ 135 - 33 \xi^2 - 23 \xi^4 - 15 \xi^6 - \frac{3}{2\xi} (1-\xi^2) (45 + 19 \xi^2 + 11 \xi^4 + 5 \xi^6) \ln \frac{1+\xi}{1-\xi} \right\} \quad (4.23)$$

and

$$\xi = \left[(1-x)^2 + 4x (\mu^2/m_p^2) \right]^{-\frac{1}{2}} (1-x) . \quad (4.24)$$

The function $h(x)$ satisfies

$$h(0) = 1 \quad \text{and} \quad h(1) = \frac{12}{105} \left(\frac{m_p}{2\mu} \right)^6 . \quad (4.25)$$

Similarly to (4.1), one may regard the physical neutron as being composed of

$$n = (N X^0) + (N 2\pi) + (\Sigma K \pi) + \dots \quad (4.26)$$

which can be obtained from (4.1) through the usual charge symmetry operation. In this simple model of the physical neutron, the constituents in the two-body channel are all neutral; thus, only the multi-body channel can contribute to structure functions in the deep inelastic $e n$ scattering. One finds

$$(W_1)_n = \beta_n F_{II}(x) . \quad (4.27)$$

The parameter β_n is related to the probability of finding a charged baryon in the

multi-particle channel of the physical neutron state, and the parameter β_p is related to the corresponding probability in the physical proton state. The ratio (β_p/β_n) depends on the detailed SU_3 structure of the multi-particle channel. For example, in the three-body channel, if the two mesons are in a pure octet state then (β_p/β_n) should lie within a range $0.58 < (\beta_p/\beta_n) < 1.8$.

In the multi-particle channel, since the bare mesons can carry charge, there must also be diagrams in which the photon is absorbed by the bare meson. These diagrams lead to a non-vanishing longitudinal structure function W_L . The magnitude of W_L depends on the bound state amplitude g'' in which only the relevant bare charged meson is off the mass shell while all other constituents, mesons and baryons, are on their mass shells. The ratio

$$\eta = \left\langle \frac{g''}{g'} \right\rangle_{Av} \quad (4.28)$$

is a free parameter in the simple phenomenological approach, though it should be computable if one knew the correct potential and, in addition, could solve the corresponding Bethe-Salpeter equation. Since the present experimental value of W_L , at least for ep scattering, is quite small and uncertain, we shall assume, for simplicity,

$$|\eta| \ll 1. \quad (4.29)$$

For a comparison with the present experimental value, we set in F_I , Eq. (4.21), the value for m_X to be simply the observed X^0 mass $\cong 958$ MeV, and in F_{II} , Eq. (4.22), the value for (μ^2/m_p^2) to be

$$\frac{\mu^2}{m_p^2} = \frac{3m_\pi^2 + 4m_K^2 + m_\eta^2}{3m_\Sigma^2 + 2m_N^2 + 2m_\Xi^2 + m_\Lambda^2} \cong .12 \quad (4.30)$$

which represents in an approximate way its SU_3 average over different three-body states $P\pi\pi$, $\Sigma K\pi$, etc. In Figure 8, the theoretical curve for $(W_1)_p$ is plotted by choosing

$$\beta_p = .22 \quad \text{and} \quad \alpha_p = 1.4 \quad (4.31)$$

The corresponding ratio for $(W_1)_n/(W_1)_p$ is plotted in Figure 9 by assuming as a simple choice

$$\beta_p = \beta_n \quad (4.32)$$

which means that in the multi-particle channel, the probability of finding a charged bare baryon in the physical nucleon state is almost independent of the total charge of the physical state p or n .

We recall that, as shown in section II, in the simple model where the physical proton consists of only the two-body channel PX^0 , the (vW_2) function satisfies an Adler sum rule (2.53); furthermore, since in that simple model $vW_2 = 2 \times m_p W_1$, Eq. (2.53) may also be written as

$$2m_p \int_0^1 dx (W_1)_p = 1 \quad (4.33)$$

In the present case, because of multi-particle channels, the integral $\int_0^1 dx (W_1)_p$ diverges, and therefore Eq. (4.33) cannot possibly hold. [Apart from other reasons,

the assumption of no subtraction constant for the dispersion integral is clearly not valid here, unlike in the simple case of a two-body bound state discussed in section II.] However, if one chooses $\beta_p = \beta_n$, then the difference $(W_1)_p - (W_1)_n$ depends only on the PX^0 channel; in this case one may define

$$\xi \equiv 2m_p \int_0^1 dx \left[(W_1)_p - (W_1)_n \right]. \quad (4.34)$$

Heuristically, ξ may be regarded as the probability for finding the PX^0 channel in the physical proton state. Thus, ξ should lie between 0 and 1. For the choice of parameters given by (4.31) and (4.32), $\xi \cong 0.17$. In the simple model where the physical nucleon consists of only the two-body channel PX^0 , or NX^0 , one has $(W_1)_n = 0$ and $\xi = 1$. Equation (4.34) then reduces to the sum rule (4.33).

B. Second example

So far we have neglected the possibility of a two-body channel in which the meson can also be charged, such as $(N\pi^+)$, $(\Sigma^0 K^+)$, etc. The inclusion is straightforward; it leads to, instead of (4.20) and (4.27),

$$(W_1)_p = \beta_p \left[F_{II}(x) + \alpha_p F_I(x) + \alpha'_p F'_I(x) \right] \quad (4.35)$$

and

$$(W_1)_n = \beta_n \left[F_{II}(x) + \alpha'_n F'_I(x) \right] \quad (4.36)$$

where α'_p and α'_n are new parameters,

$$F'_I(x) = (1-x)^3 \frac{m_p^4 \left[m_p^2(1-x)^2 + \frac{1}{3} \mu^2 x \right]}{\left[m_p^2(1-x)^2 + \mu^2 x \right]^3} \quad (4.37)$$

and μ^2/m_p^2 is given by (4.30). We note that, as $x \rightarrow 0$, $(W_L)_n/(W_L)_p$ now approaches a non-zero constant. The presence of such new two-body states will also give a new contribution to the W_L function. The magnitude of this W_L function depends on the two-body wave function g''' in which the charged meson is off-mass-shell, but the baryon is on-mass-shell. It is easy to see that g''' should have a similar asymptotic behavior as that of $g(u)$ given in (4.9). If one assumes, similarly to (4.10),

$$g''' \propto (u + \mu^2)^{-1} \quad (4.38)$$

then the resulting W_L function is proportional to

$$F_L(x) = \frac{x(1-x)^2 [m_p^2 x^2 + \frac{1}{3}\mu^2(1-x)]}{[m_p^2 x^2 + \mu^2(1-x)]^3} \quad (4.39)$$

Equation (4.39) shows that the threshold relation which we have derived for spin $\frac{1}{2}$ charged constituents and the transverse structure function is not, however, valid for spin 0 constituents for the longitudinal structure function. For interactions with both nucleon and pion currents, the elastic form factor decreases¹⁰ as $1/q^4$; but Eq. (4.39) shows only a quadratic threshold behavior $(1-x)^2$ for W_L as $x \rightarrow 1$. That W_L must be an even function of $(1-x)$ near threshold was already proved in Ref. 6. At present, the experimental data is consistent with $\alpha'_p \cong \alpha'_n \cong 0$.

We showed in our Bethe-Salpeter analysis that structure functions measure the wave function of the bound state. In this section we have now shown that a simple guess of the wave function can provide a qualitative fit to the data.

V. Comments

A. The physical bound-state model that we have developed in sections II and III avoids some of the formal difficulties of the parton model. It is Lorentz invariant and relativistically covariant at each step of the development, not just at the infinite momentum scaling limit. It provides a physical connection between the observations of scaling of the structure functions in deep inelastic scaling and of rapid decrease of the electromagnetic form factors in elastic scattering. It also reveals the relation between the bound-state wave function of the proton for large momenta, i.e., $g(u) \sim O(u^{-1})$, and the threshold behavior of $W_1 \sim O[(1-x)^3]$ near $x = 1$ as well as its crossing property to the annihilation channel. In addition, since the bound state is constructed of a few (two or three) constituents of masses $\lesssim 1$ GeV there is no large parameter $> (1 \text{ GeV})^2$ against which to measure $m_p v$ or q^2 in approaching the scaling region. This model gives then a qualitative understanding of the fact that in ep inelastic scattering the scaling property is already observed at relatively moderate energies.

In the context of this model we may ask what will be the behavior of inelastic transitions induced by very virtual photons to specific final states (e.g., " γ " + $p \rightarrow \Delta$, or $\rightarrow p + \pi$, etc.). In order to form such states it is necessary to add specific final state interaction channels such as illustrated schematically in Figure 10 for " γ " + $p \rightarrow p$ + some fixed meson channel. Aside from spin factors and their accompanying numerator polynomials, the amplitude for this graph will have the same asymptotic behavior for large q^2 as in Figure 2 for the elastic form factor. The large momentum q can ride along the virtual bare proton line, marked P' , in

both diagrams since the proton's decreasing wave functions introduce more than enough powers of momentum to converge the loop integrals. Therefore, the added propagator and vertices connected with meson wave functions in Figure 10 have no effect on the power dependence of the asymptotic behavior; aside from spin factors²², the structure functions for such "exclusive" reactions will show form factors decreasing with²³ increasing q^2 .

B. The bound-state model constructed in the previous sections can also be applied to calculating additional observables—in particular spin-dependent effects for scattering of polarized electrons from polarized targets²⁴ and neutrino and antineutrino deep inelastic cross sections. Near the threshold region, i.e., near $x = 1$, the two-particle state of (PX^0) will dominate in our model due to the threshold factor of $(1-x)^3$ relative to the $(1-x)^5$ factor for the three-particle contributions. In the scaling region it contributes a large polarization asymmetry A , defined as the difference divided by the sum of cross sections for parallel and antiparallel spin directions of the incident electron relative to the target nucleons. Let E_1 and E_2 be, respectively, the electron energies in the laboratory before and after scattering, and θ the scattering angle. One finds using $g = (u + m_p^2)^{-1}$

$$A = \frac{d\sigma_{\uparrow\uparrow} - d\sigma_{\uparrow\downarrow}}{d\sigma_{\uparrow\uparrow} + d\sigma_{\uparrow\downarrow}} = \left\{ \frac{E_1 + E_2}{v + x m_p \cos^2 \theta/2} \right\} \left\{ \frac{3(1-x)^2 - x \frac{\mu^2}{m_p^2}}{3(1-x)^2 + x \frac{\mu^2}{m_p^2}} \right\} . \quad (5.1)$$

The first factor is essentially kinematical; the second one is limited in magnitude to be less than unity by positivity conditions²⁵ on the structure functions when $W_L = 0$,

as it is in this model with a spin $\frac{1}{2}$ charged constituent. One sees that the asymmetry depends sensitively on the parameter (μ/m_p) . For $(\mu/m_p) \ll 1$, the second factor is close to unity for $0 \leq x < 1 - O(\mu/m_p)$, dropping rapidly to zero at $x \cong 1 - 3^{-\frac{1}{2}}(\mu/m_p)$ and then reversing sign. For a single free spin $\frac{1}{2}$ constituent we would expect the asymmetry to be unity; the above behavior reflects the very massive virtual character of the intermediate constituent that is apparent in (2.39) as $x \cong 1$. For small x values we must also include the three-particle wave function and our model predicts maximal asymmetry if there are no charged zero-spin constituents and $W_L = 0$. For neutrino processes we find near $x \sim 1$, in analogy with the proton-neutron ratio shown in Figure 9, that the ν to $\bar{\nu}$ ratio on proton targets vanishes. This is because the bare proton constituent can lower but not raise its charge by one unit by absorbing a negatively charged intermediate boson W^- as $\bar{\nu} \rightarrow e^+ + W^-$, but not a positively charged intermediate boson W^+ as $\nu \rightarrow e^- + W^+$. The prediction of spin asymmetries and of ν , $\bar{\nu}$ differences can be further refined in terms of the ratio, R , of longitudinal to transverse photon interactions which we have for simplicity set to zero in the present analysis.

C. As we shall discuss in the following, there remain several important questions whose answers lie outside the scope of the present model. In common with all parton (and quark) models, there exists the difficult problem of "Where and what are the constituents that are bound together forming the physical nucleon?". Since these constituents are assigned point-like electromagnetic vertices, in order to give a meaningful calculation for the structure functions and electromagnetic form factors of the physical nucleon, they differ from observed hadrons (viz., nucleons and their

low-lying resonances; pions, etc.). We have no complete or persuasive theory of the nature and reality of these constituents. Nevertheless, it seems reasonable to think that they should "dress" themselves before emerging, as illustrated by the schematic diagram given in Figure 10. According to this picture, the asymptotic state describing the initial hadronic state at time $T \rightarrow -\infty$ is the physical proton. At any finite time T when the virtual photon hits, it interacts only with the bare charged constituents. These bare constituents are not, however, contained in the complete spectrum of asymptotic free-particle states emerging at $T \rightarrow +\infty$ after the scattering. To answer the question as to what is going on dynamically in the outgoing region, one needs to construct a more complete theory, and this we are not proposing to do here.

The problem that we are facing is not a new one in physics. It occurs, for example, in nuclear physics. The deuteron is a stable bound state, and has as its bound constituents the neutron and proton; however, when the neutron emerges from a disintegrated deuteron, it decays in ≈ 18 minutes. Because of the weak binding of the deuteron ($\sim 0.1\%$ packing fraction) and the long decay time of the neutron due to the weakness of the β -decay coupling, there is no difficulty in understanding the physical processes involved. However, when we study the dynamics of the proton's structure we are up against strong binding ($\approx 100\%$ packing fraction) and presumably very short "dressing times", or "decay times", for the constituents so that simple approximate intuitive physical pictures fail us. Nevertheless, as a formal solution, one may adopt the naive approach that the bare constituents are simply ordinary unstable particles. For example, this instability may be caused by

postulating the bare constituents to be somewhat heavier, say within a factor of two, than the corresponding physical particles; in addition, their decays are assumed to be extremely fast so as to escape detection. Such an approach is clearly formally sound, though physically unsatisfactory.

As an alternative suggestion, one may adopt the physically attractive picture that the relation between a bare constituent and its corresponding physical "composite" particle is almost identical to that between a bare particle and a physical "elementary" particle in the usual field theory. The bare particles have point-like vertices, while the physical particles have q^2 -dependent form factors; both the spectrum of all bare particles and the spectrum of all physical particles are complete, and therefore any calculation of the total cross section summing over all final channels of physical particles can also be obtained by summing over all final channels of bare particles. The bare particle concept is useful in the Heisenberg equation of motion description, since on account of their point-like vertices the interactions between bare particles are local; however, in terms of observations in the asymptotic region of a collision process, only the physical particles actually emerge. At present, it is still an open question as to how one might develop a complete theory, so that such relations could indeed exist between the bare constituents and their corresponding physical composites.

D. The question of final state multiplicity is an important one, though it is clear that no complete answer is possible unless the question raised in the preceding comment is resolved. Nevertheless, it is conceivable that some partial answers could be derived by using, for example, the simple (and artificial) field-theory model in which all bare particles are described by elementary fields and the bare nucleon is

regarded simply as an unstable particle. [If one wishes, one may either regard the bare mesons as the physical ones except for renormalizations, or as unstable particles like the bare nucleon.] There are then at least three different mechanisms that might contribute to final state multiplicity: (i) the multi-particle bound-state channels in the physical nucleon state, such as the $(P \pi \pi)$, $(\Sigma K \pi)$ channels discussed in section IV, (ii) the decay of the bare nucleon after its separation from the physical composite system and (iii) the radiation of additional quanta (called gluons for convenience, as in section II.F) associated with whatever fields are responsible for the binding potential for the bound state. For large values of $s = -(p+q)^2$, the first two mechanisms are expected to lead to a final state multiplicity independent of s , while the third mechanism, at least for soft quanta radiation and in the eikonal approximation, might give a final state multiplicity that increases logarithmically with s . One may then conjecture that the total final state multiplicity N in, say, $e p$ inelastic scattering is approximately given by, for large s ,

$$N = a(x) + b(x) \ln (s/m) \quad (5.2)$$

where $a(x)$ and $b(x)$ are independent of s but depend on the scaling variable x as well as on the nature of the particular physical particle under consideration, such as the pion multiplicity or the kaon multiplicity.

In the simple bound-state model considered in this paper only the above mechanism (i) is explicitly taken into account. It is clear that mechanism (ii) does not alter the (total) deep inelastic cross-section, since one sums over all final hadronic channels. With respect to mechanism (iii) the over-all picture has a familiar analogue in atomic physics, in which case the quantum responsible for the binding force is the electro-

magnetic radiation. One may either simply ignore the final photon radiation and directly evaluate the cross section for, say, the photo-disintegration of the atom, or one may do the same calculation, but properly take into account all final soft photon radiation. Under the Bloch-Nordsieck approximation, these two approaches lead to the same cross section, provided all final channels are summed over.

The above remark is correct if one includes only soft radiation. In the case of atomic physics, the inclusion of hard photons in the final state would lead to departures from the Bloch-Nordsieck approximation; in the present case, as we shall discuss, it may lead to violations of the scaling property.

E. We now turn to another important question: whether the scaling property is an exact law of nature in the high energy (scaling) limit, or just an approximate one which holds only in some intermediate energy range. For definiteness, let us consider the forward Compton scattering amplitude. As shown in section II. F, under the ladder approximation, the absorptive part due to those on-mass-shell intermediate states consisting of the bare constituents plus a number of gluons can be neglected in the scaling limit. As a generalization of the ladder approximation we may also include crossed graphs; i.e., diagrams in which the gluons being exchanged between different bare constituents are absorbed and emitted in arbitrary sequence. If the contribution of these crossed graphs is calculated iteratively using a bound-state wave function based on a ladder model that satisfies (1.3), it is not difficult to see that the same conclusion holds and the radiation of real gluons can be neglected.

If these were the only diagrams, then the scaling property could be an exact

law. However, there are other diagrams, such as those connected with renormalizations in which the gluons are exchanged between the same bare constituent. Unlike the case of either ladder diagrams or soft radiation, these gluon renormalization and radiative correction diagrams are typically divergent in the ultra-violet region.

If or when these gluon renormalization contributions become important we may expect deviations to occur from the scaling prediction. On the one hand, they may behave in analogy to the case of electromagnetic radiative corrections, where it is known that there should be deviations from the scaling property $\sim 0 [\alpha \ln (q^2/m^2)]$; in the case that the gluon is, say, a spin 0 meson, since the renormalization diagrams have the same logarithmic divergence as the corresponding electromagnetic ones, one may expect a similar deviation from the scaling property $\sim 0 [\epsilon \ln (q^2/m^2)]$. The magnitude of ϵ is proportional to the probability of hard gluon (or meson) radiation, which can be rather small. The present experimental data is consistent with $\epsilon \lesssim 10^{-1}$. In any case, just based on the electromagnetic radiative correction, one should have $\epsilon \geq \alpha$. The scaling property is, therefore, not an exact one in the mathematical high energy limit, but is only approximately valid in the range including the one presently accessible to experimental study

$$1 < q^2 \text{ in } (\text{GeV})^2 < \exp(\epsilon^{-1}) \leq \exp(\alpha^{-1}). \quad (5.3)$$

Alternatively, the possibility remains that the sum total of the gluon radiative corrections may be, simply, to give rise to a form factor of the constituent itself that decreases with increasing momentum transfer q and tends to zero for large q^2 in

analogy to the observed hadronic structure. If such is the case, we may expect to observe modifications from scaling leading to structure functions decreasing at sufficiently high momentum transfers q^2 such that $q^2 \langle R^2 \rangle$ is not longer negligible where $\langle R^2 \rangle$ denotes a mean square radius of the charge constituents (i.e., "bare" particles). Evidently the extension of the kinematic range of experimental study for the structure functions will be of exceedingly great interest and importance.

F. Although the physical description and motivation of the bound-state model described in this paper are very different, there are related studies of the proton's structure in deep inelastic scattering that have similar mathematical features. In particular, Landshoff, Polkinghorne and Short²⁶ present a parton model in which the virtual photon is assumed to be absorbed on a point-like parton current and the physical input is given in terms of the properties of the parton-proton scattering amplitude. Their major assumption is that the off-mass-shell parton-proton scattering amplitude decreases sufficiently rapidly with increasing parton mass. In their model this assumption provides the necessary convergence properties that we introduced via the wave function $g(u) \sim 1/u$ in our bound-state model.

The phenomenological model of West²⁷ is very much in the same spirit as this. Again it introduces electromagnetic interactions with point-like partons and makes a convergence or "smoothness" assumption on the parton-proton scattering amplitude. West derives in this way the same relation between elastic and inelastic structure functions that we have given earlier. What is introduced as the dependence of the parton-proton scattering amplitude on the mass of the virtual parton in West's approach corresponds to the bound-state wave function of the physical proton in our approach.

We wish to thank J. D. Bjorken and S. B. Treiman for stimulating discussions. One of us (T. D. L.) wishes to thank E. M. Henley and other members of the Physics Department at the University of Washington for helpful discussions and for their kind hospitality extended to him in the summer of 1971, during which the early part of this work was done.

Appendix A

In this Appendix, we shall show that the Fourier transform of the ground-state wave function $\psi_p(k)$ is regular at the origin in the coordinate space $x = 0$, and therefore

$$\int \psi_p(k) d^4k \quad \text{is finite.} \quad (\text{A.1})$$

It is convenient to start with the Bethe-Salpeter equation (2.12). For simplicity, let us consider the special case

$$\mu = M \quad \text{and} \quad m_p = 0 \quad ; \quad (\text{A.2})$$

i.e., the bound state is of zero mass and its two constituents P and X^0 are of the same mass M . [It is straightforward, though somewhat tedious, to extend the arguments given below to the general case $\mu \neq M$ and $m_p \neq 0$.]

Following Wick²⁰, we first rotate the real axis in the complex k_0 -plane counter-clockwise to the imaginary axis, thus changing k_0 real to $k_0 = i k_4$ imaginary. By using (A.2) and by setting the total 4-momentum $p_v = 0$, one may write Eq. (2.12) in the Euclidean space as

$$\left(\gamma_v \frac{\partial}{\partial x_v} + M \right) \left(\frac{\partial^2}{\partial x_\mu^2} - M^2 \right) \tilde{\Gamma}(x) = -\lambda \tilde{V}(x) \tilde{\Gamma}(x) \quad (\text{A.3})$$

where $\tilde{V}(x)$ and $\tilde{\Gamma}(x)$ are, respectively, the Fourier transforms of $V(k)$ and $\Gamma_{p=0}(k)$

$$\tilde{V}(x) = \int V(k) e^{i k \cdot x} [d^4k] \quad (\text{A.4})$$

$$\tilde{\Gamma}(x) = \int \Gamma_{p=0}(k) e^{i k \cdot x} [d^4 k] \quad (A.5)$$

and $[d^4 k] = dk_1 dk_2 dk_3 dk_4$ is real. The spinor dependence of $\tilde{\Gamma}(x)$ can be separated by introducing two c-number functions $f_1(x)$ and $f_2(x)$:

$$\tilde{\Gamma}(x) = f_1 \gamma_5 + M^{-1} \left(\gamma_\mu \frac{\partial}{\partial x_\mu} \right) f_2 \gamma_5 \quad (A.6)$$

in which the factor γ_5 is due to the assumed pseudoscalar nature of X^0 . If X^0 were a scalar, then γ_5 would be replaced by unity. For the ground state, f_1 and f_2 depend only on

$$r = (x_1^2 + x_2^2 + x_3^2 + x_4^2)^{\frac{1}{2}}. \quad (A.7)$$

Eq. (A.2) reduces then to two coupled ordinary differential equations

$$\left(\frac{d^2}{dr^2} + \frac{3}{r} \frac{d}{dr} - M^2 \right) [M^2 f_1 + \left(\frac{d}{dr} + \frac{3}{r} \right) f_2'] = -\lambda M \tilde{V} f_1$$

and (A.8)

$$\left(\frac{d^2}{dr^2} + \frac{3}{r} \frac{d}{dr} - M^2 - \frac{3}{r^2} \right) \left[\frac{df_1}{dr} + f_2' \right] = -\lambda M^{-1} \tilde{V} f_2'$$

where (A.9)

$$f_2' = \frac{df_2}{dr}.$$

From (A.6), one sees that $\tilde{\Gamma}(x)$ depends only on f_1 and f_2' , but not on f_2 explicitly. Since both equations in (A.8) are of third order in (d/dr) , there should be six independent solutions for $\tilde{\Gamma}(x)$.

According to the standard procedures for the eigenvalue problem of a Sturm-Lionville equation, in order to determine whether the eigenstate $\tilde{\Gamma}(x)$ is regular at $r = 0$ or not, one has to show that (A.8) has three regular solutions at $r = 0$, say Γ_1 , Γ_2 , Γ_3 , and three regular solutions at $r = \infty$, say Γ_a , Γ_b and Γ_c . The bound state $\tilde{\Gamma}(x)$ can be written as a sum

$$\tilde{\Gamma}(x) = \alpha \Gamma_1 + \beta \Gamma_2 + \Gamma_3 \quad . \quad (\text{A.10})$$

one then adjusts the three parameters α , β and the eigenvalue λ so that $\tilde{\Gamma}(x)$ is regular at $r = \infty$; i.e.

$$\tilde{\Gamma}(x) = \alpha \Gamma_a + b \Gamma_b + c \Gamma_c \quad . \quad (\text{A.11})$$

To show that there are three regular solutions at $r = \infty$, let us assume, for simplicity, the covariant potential V to be superpositions of Yukawa-like forms with non-zero masses [i.e., in (1.1), $\sigma(\kappa^2)$ is not proportional to $\delta(\kappa^2)$]. Therefore, as $r \rightarrow \infty$, $\tilde{V} \rightarrow 0$ exponentially. At large r (A.8) becomes simply the free equation. One can readily verify that for $V = 0$ the six independent solutions consist of three regular ones

$$(a) \quad f_1 = r^{-1} H_1^{(1)}(i M r) \rightarrow \text{constant} \cdot r^{-3/2} \exp(-M r),$$

$$f_2' = - \frac{df_1}{dr}$$

$$(b) \quad f_1 = 0 \quad ,$$

$$f_2' = r^{-1} H_2^{(1)}(i M r) \rightarrow \text{constant} \cdot r^{-3/2} \exp(-M r)$$

$$(c) \quad f_1 = r^{-1} G_1^{(1)}(i M r) \rightarrow \text{constant} \cdot r^{-\frac{1}{2}} \exp(-M r)$$

$$f_2' = - \frac{df_1}{dr} ,$$

and three irregular ones

$$(d) \quad f_1 = r^{-1} H_1^{(2)}(i M r) \rightarrow \text{constant} \cdot r^{-3/2} \exp(M r)$$

$$f_2' = - \frac{df_1}{dr}$$

$$(e) \quad f_1 = 0$$

$$f_2' = r^{-1} H_2^{(2)}(i M r) \rightarrow \text{constant} \cdot r^{-3/2} \exp(M r)$$

and

$$(f) \quad f_1 = r^{-1} G_1^{(2)}(i M r) \rightarrow \text{constant} \cdot r^{-\frac{1}{2}} \exp(M r)$$

$$f_2' = - \frac{df_1}{dr}$$

where $H_1^{(1)}$, $H_1^{(2)}$, $H_2^{(1)}$ and $H_2^{(2)}$ are the standard Hankel functions²⁸, and $G_1^{(i)}$ ($i = 1$ or 2), besides satisfying the above asymptotic behavior, is also the solution of the following inhomogeneous Bessel equation:

$$\left[\frac{d^2}{dz^2} + \frac{1}{z} \frac{d}{dz} + \left(1 - \frac{1}{z^2}\right) \right] G_1^{(i)}(z) = H_1^{(i)}(z) \quad (A.12)$$

Our next task is to investigate the behavior at small r . On account of

(1.2), as $r \rightarrow 0$, \tilde{V} is proportional to r^{-2} . Without any loss of generality, we may choose $M = 1$ and define the coupling constant λ so that

$$\tilde{V} \rightarrow 4 r^{-2} \quad \text{as} \quad r \rightarrow 0. \quad (\text{A.13})$$

As we shall see, as $r \rightarrow 0$ there are indeed three regular solutions given by

$$(i) \quad f_1 \rightarrow c_1 r^2, \quad f_2' \rightarrow c_2 r^3$$

$$(ii) \quad f_1 \rightarrow c_1 r^2 \ln r, \quad f_2' \rightarrow c_2 r$$

and $(iii) \quad f_1 \rightarrow c_1, \quad f_2' \rightarrow c_2 r \ln r;$

in addition there are three irregular solutions

$$(iv) \quad f_1 \rightarrow c_1 \ln r, \quad f_2' \rightarrow c_2 r^{-1}$$

$$(v) \quad f_1 \rightarrow c_1 r^{-2}, \quad f_2' \rightarrow c_2 r^{-1} \ln r$$

and

$$(vi) \quad f_1 \rightarrow c_1 r^{-2} \ln r, \quad f_2' \rightarrow c_2 r^{-3}.$$

where c_1 and c_2 denote the appropriate constants.

The derivation of these results follows the standard method. The first regular solution is obtained through the usual indicial equation by expanding f_1 and f_2' as power series in r . One finds

$$f_1 = s(r) = r^2 \sum_0^{\infty} s_n r^{2n} \quad (A.14)$$

$$f_2' = t(r) = r^3 \sum_0^{\infty} t_n r^{2n}$$

To obtain the second regular solution, one assumes f_1 and f_2' to be given, respectively, by $\ln r$ times the first regular solution plus a power series in r .

The result is

$$f_1 = (\ln r) s + r^4 \sum_0^{\infty} a_n r^{2n}$$

and

$$f_2' = (\ln r) t + r \sum_0^{\infty} b_n r^{2n} \quad (A.15)$$

where s and t are given by (A.14) and a_n, b_n can be easily determined by substituting (A.15) into (A.8).

To derive the third regular solution, one assumes

$$f_1 = (\ln r)^2 s + (\ln r) u_1 + v_1 \quad (A.16)$$

and

$$f_2' = (\ln r)^2 t + (\ln r) u_2 + v_2$$

where u_i and v_i ($i = 1$ and 2) are power series in r . It can be readily verified that these power series expansions are of the form

$$u_1 = r^4 \sum_0^{\infty} (u_1)_n r^{2n}, \quad v_1 = \sum_0^{\infty} (v_1)_n r^{2n}$$

$$u_2 = r \sum_0^{\infty} (u_2)_n r^{2n} \quad \text{and} \quad v_2 = r \sum_0^{\infty} (v_2)_n r^{2n} \quad (A.17)$$

More explicitly, this third regular solution is given by, as $r \rightarrow 0$,

$$f_1 \rightarrow 1 + \frac{1}{8} \lambda^2 r^2 (\ln r)^2 + o(r^2)$$

and

(A.18)

$$f_2 \rightarrow -\frac{1}{2} \lambda r \ln r + \frac{1}{8} (-3\lambda + 4) r - \frac{1}{96} \lambda^2 (\lambda + 2) r^3 (\ln r)^2 + o(r^3 \ln r).$$

According to (A. 10), the bound-state wave function is a linear function of the above three regular solutions, (A. 14)-(A. 16). From the explicit form of these solutions, one sees that as $r \rightarrow 0$ the third regular solution dominates over the other two; thus, (A. 18) holds for the bound-state wave function as well. By using (A.6) and (A.18) one sees that $\tilde{\Gamma}(0)$ exists, and therefore, on account of (2. 10),

$$\psi_p(k) = \Gamma_p(k) u_p,$$

the Fourier transform of the bound-state wave function $\psi_p(k)$

$$\tilde{\psi}_p(x) \equiv \int \psi_p(k) e^{ik \cdot x} d^4 k \quad (A.19)$$

is regular at the origin; consequently, (2.8) and (2.9) hold.

We note that in a 4-dimensional Euclidean space the Fourier transform of any function $h(r)$, regular at both $r = 0$ and ∞ , satisfies

$$\int e^{ik \cdot x} h(r) d^4 r = -4\pi^2 k^{-4} \int_0^\infty J_0(kr) [3h' + 5r h'' + r^2 h'''] dr \quad (A.20)$$

where J_0 is the zeroth order Bessel function. Thus, for example, by setting

$h = f_2$, which according to (A. 18) is

$$c = \frac{1}{4} \lambda r^2 \ln r + O(r^2)$$

where c is a constant, and by using (A. 20), one finds that, through partial integration, as $k^2 \rightarrow \infty$

$$\int e^{i\mathbf{k} \cdot \mathbf{x}} f_2 d^4r = -16\pi^2 \lambda k^{-6} + O(k^{-8}) . \quad (\text{A.21})$$

It is then straightforward to show that as $k^2 \rightarrow \infty$ the bound state solution

$\Gamma_p(k)$ satisfies

$$\Gamma_p(k) = \text{constant } (-i\gamma \cdot k) \gamma_5 k^{-6} + O(k^{-6} \ln k^2) \quad (\text{A.22})$$

The explicit form (A. 18) enables one to determine not only the leading behavior, but also the form of the next order correction term $O(k^{-6} \ln k^2)$. By using (A. 22), one may also directly establish (2.9) and (2.37).

Appendix B

To establish the identity (2.21), one may first differentiate both (2.6) and (2.16) with respect to k_v , keeping p_v fixed; next multiply them, respectively, by $\bar{\psi}_p(k) = \bar{\phi}_p(k) K_p^{-1}(k)$ on the left and $\psi_p(k) = K_p^{-1}(k) \phi_p(k)$ on the right; and then add these two equations together. This leads to

$$\begin{aligned}
 & \int \bar{\phi}_p(k) \left[\frac{\partial K_p^{-1}(k)}{\partial k_v} \right]_p \phi_p(k) d^4k \\
 &= -i\lambda \int \bar{\psi}_p(k) \psi_p(k') \left[\frac{\partial}{\partial k'_v} + \frac{\partial}{\partial k_v} \right] V(k-k') d^4k d^4k' \\
 &= 0,
 \end{aligned} \tag{B.1}$$

and, therefore, (2.21) is proved.

To establish (2.22), one may first differentiate (2.6) with respect to p_v , keeping k_v fixed; next multiply on the left by $\bar{\psi}_p(k)$; and then integrate over d^4k . After using (2.16), one finds

$$\begin{aligned}
 \int \bar{\psi}_p(k) \left[\frac{\partial K_p(k)}{\partial p_v} \right]_k \psi_p(k) d^4k &= i \frac{\partial \lambda}{\partial p_v} \int \bar{\psi}_p(k) V(k-k') \psi_p(k') d^4k d^4k' \\
 &= \frac{\partial \ln \lambda}{\partial p_v} \int \bar{\psi}_p(k) K_p(k) \psi_p(k) d^4k.
 \end{aligned} \tag{B.2}$$

Since $\lambda = \lambda(m_p^2)$ and

$$\left[\frac{\partial}{\partial p_v} K_p(k) \right]_k + \frac{\mu}{M+\mu} \left[\frac{\partial}{\partial k_v} K_p(k) \right]_p = \left[\frac{\partial}{\partial p_v} K_p(k) \right]_X = -i\gamma_v (X^2 + \mu^2);$$

(2.22) follows on account of (B.2), (2.20) and (2.21).

Appendix C

In this appendix, we give the detailed derivation of why the amplitude I_V^1 , defined by (2.32), can be neglected in the scaling limit. It is useful to determine in (2.32) the integration domain in which the integrand does not approach zero in the scaling limit. Let us first examine the denominator. We observed that because of the wave function $\phi_p(k_{in})$ and the propagators $[-i \gamma \cdot (p - X') - M]^{-1} [X'^2 + \mu^2]^{-1}$ in the integrand in (2.32) this domain is restricted to

$$X'^2 = 0(m^2) \quad \text{and} \quad (p - X')^2 = 0(m^2), \quad (C.1)$$

and because of the denominator in the propagator

$$[-i \gamma \cdot P' - M]^{-1} = -[P'^2 + M^2]^{-1} [-i \gamma \cdot P' + M] \quad (C.2)$$

there is the additional constraint

$$P'^2 = (p + q - X')^2 = 0(m^2) \quad (C.3)$$

where m denotes collectively the relevant masses m_p , M and μ . In the laboratory frame, the first two constraints (C.1) imply that each of the four components of X'_μ should be restricted to

$$X'_\mu = 0(m). \quad (C.4)$$

The additional constraint (C.3) then implies that in the scaling limit of $q^2 \rightarrow \infty$, $-(p \cdot q) \rightarrow \infty$ but keeping the scaling variable

$$x = q^2 / (-2p \cdot q) \quad \text{finite}, \quad (C.5)$$

the components X_3' and X_0' are further related by

$$X_0' - X_3' = (1-x) m_p + 0 \left(\frac{m^3}{q^2} \right) \quad (C.6)$$

where the z-axis is chosen to be parallel to \underline{q} . These constraints (C.4) and (C.6) restrict the integration region of interest to a volume

$$\int d^4 X' = 0(m^6/q^2); \quad (C.7)$$

in this region, all denominators in the integrand of (2.32) are finite in the scaling limit.

Next, we have to determine in this region the magnitude of the numerator in (2.32).

On account of (2.33) and (1.2), at large 4-momentum-transfer-squared $(k' - k)^2$ the scattering matrix $\langle k | T_{p+q} | k' \rangle$, like $V(k' - k)$, decreases as $(k' - k)^{-2}$. This, together with (C.4) and (C.6), implies that in the laboratory frame the final 4-momenta are restricted to

$$X_\mu = 0(m) \quad \text{and} \quad P_\mu = q_\mu + 0(m).$$

Since the virtual momentum $P'_\mu = q_\mu + 0(m)$ as well, in the integral (2.32), after using (C.2), one has the numerator factor

$$u_P^\dagger \gamma_4 \langle k | T_{p+q} | k' \rangle (-i \gamma \cdot P' + M) = \\ \langle K | T_{p+q} | k \rangle u_P^\dagger \gamma_4 (-i \gamma \cdot P + M) + 0(m),$$

which is also $0(m)$. Therefore, one finds that the integrand in (2.32) remains finite in the integration region (C.7) and, consequently, the integral over this region is proportional to the volume which approaches zero in the scaling limit. Outside this

region (C.7), the integrand itself approaches zero at least as $O(q^{-2})$; furthermore, the corresponding integral is dominated by the region in which (C.4) remains valid, but, in place of (C.3), $P'^2 = O(q^2)$. Since the integration over X' is a superconvergent one, the integral (2.32) remains convergent (in fact remains superconvergent) if the propagator with the large virtual momentum P' is taken outside the integral. It then follows that the entire integral I'_V goes to zero in the scaling limit and therefore can be neglected.

Appendix D

To establish (2.52) it is convenient to start from (2.51) and to use the laboratory frame with the z -axis parallel to \underline{q} . One has then

$$\text{and} \quad U_1 = F_{11} = F_{22} \quad (\text{D.1})$$

$$v U_2 = \frac{v q^2}{v^2 + q^2} \left[F_{11} + \frac{q^2}{v^2} F_{33} \right] .$$

It is easy to see that in the scaling limit F_{33} remains finite, and therefore $v U_2 \rightarrow 2 \times m_p U_1$. Consequently, one needs only to investigate F_{11} , or A_{11} and B_{11} . Because of the rapid convergence property of the bound-state wave function, the integral (2.47) for A_{11} is determined only by its value over the domain in which

$$X^2 = 0(m^2) \quad \text{and} \quad (p-X)^2 = 0(m^2) . \quad (\text{D.2})$$

These constraints imply that in the laboratory frame all components of X_μ are $0(m)$. Similarly, in the same laboratory frame the integral (2.48) for B_{11} is determined only by its value over the domain in which

$$X_\mu = 0(m) \quad \text{and} \quad X'_\mu = 0(m) . \quad (\text{D.3})$$

For A_{11} , the magnitude of the integrand in (2.47) is proportional to the appropriate matrix element of

$$[-i \gamma \cdot P - M]^{-1} = (P^2 + M^2)^{-1} [i \gamma \cdot q + 0(m)] \quad (\text{D.4})$$

in which the numerator on the right hand side is $0(v)$. If $P^2 = 0(q^2)$, then (D.4) is $0(m^{-1})$, and the integrand in (2.47) remains finite in the scaling limit. On the other hand, if $P^2 = 0(m^2)$, then (D.4) is $0(v/m^2)$. However, in the latter case, on account of $P^2 = (p+q-X)^2$, the components of X_μ in the laboratory frame must be further restricted to

$$X_0 - X_3 = (1-x)m_p + 0(m^2/v) ; \quad (D.5)$$

consequently, although the integrand in (2.47) is $0(v)$, the relevant integration volume $\int d^4X$ is $0(m^5/v)$. Thus, one finds that A_{11} remains finite and non-zero in the scaling limit.

To study the magnitude of B_{11} , it is convenient to use (2.33) and formally expand B_{11} as a power series in the coupling constant λ of the binding potential V . We write

$$B_{11} = \sum_{n=1}^{\infty} \lambda^n B_{11}^n \quad (D.6)$$

in which, e. g., the first term λB_{11}^1 is given by the same expression (2.48) except that $\langle k | T_{p+q} | k' \rangle$ is replaced by $i\lambda V(k' - k)$. The magnitude of the resulting integrand for B_{11}^1 is proportional to the appropriate matrix element of the product

$$\begin{aligned} [-i\gamma \cdot P - M]^{-1} [-i\gamma \cdot P' - M]^{-1} &= (P^2 + M^2)^{-1} (P'^2 + M^2)^{-1} \\ &\quad [-i\gamma \cdot P + M] [-i\gamma \cdot P' + M] . \end{aligned} \quad (D.7)$$

Because of (2.49) and (D.3), the numerator on the right hand side of (D.7) is equal to $-q^2 + 0(m) [-i\gamma \cdot q] + 0(m^2)$ which is $0(q^2)$ in the scaling limit. If $P^2 = 0(q^2)$

and $P'^2 = 0(q^2)$, then (D.7) is $0(q^{-2})$. If $P^2 = 0(m^2)$ but $P'^2 = 0(q^2)$, then (D.7) is $0(m^{-2})$ but, in addition to (D.3), the components of X_μ are further constrained by (D.5), so that the relevant integration volume $\int d^4X$ is $0(m^5/v)$. Similarly, if $P'^2 = 0(m^2)$ then the relevant integration volume $\int d^4X'$ is reduced to $0(m^5/v)$. Putting all these together, one finds that

$$B_{11}^1 \sim 0(v^{-1})$$

in the scaling limit. By following the same reasoning, it can be readily established that for $\ell \geq 1$, apart from possible $\ln(v/m)$ factors,

$$B_{11}^{2\ell} \sim 0(v^{-\ell}) \quad \text{and} \quad B_{11}^{2\ell-1} \sim 0(v^{-\ell}).$$

Thus, in the scaling limit,

$$F_{11} \rightarrow A_{11}(p, q) + A_{11}(p, -q) \quad (D.8)$$

from which, by taking the imaginary part, (2.52) follows. We note that, like the diagram I_v^1 in Figure 3, the diagram $B_{\lambda v}$ in Figure 4 is needed for maintaining gauge invariance but can be neglected in the scaling limit.

Appendix E

To complete the proof for the sum rule (2.53), we follow closely the steps taken by Adler¹⁷, making sure that all the assumptions used in the usual derivation are indeed valid in the present case. In the laboratory frame, the amplitude $F'_{\lambda\nu}$, defined by (2.54), may be written as

$$F'_{ij}(p, q) = \delta_{ij} a_1(q^2, \nu) + q_i q_j a_2(q^2, \nu) ,$$

$$F'_{i4}(p, q) = q_i b(q^2, \nu) , \quad F'_{4i}(p, q) = -q_i b(q^2, -\nu) \quad (E.1)$$

and

$$F'_{44}(p, q) = c(q^2, \nu)$$

where the subscripts i and j denote the space-components. These four functions a_1 , a_2 , b and c are related through the divergence condition (2.56). By setting the subscript λ in (2.56) to be, respectively, the time and the appropriate space components one finds that

$$\nu c - i(q^2 + \nu^2) b = 2 \quad (E.2)$$

and

$$a_1 + (q^2 + \nu^2) a_2 + i\nu b = 0 \quad (E.3)$$

in which, on account of (2.55), $a_1(q^2, \nu)$, $a_2(q^2, \nu)$ and $c(q^2, \nu)$ are odd in ν , but $b(q^2, \nu)$ is even in ν .

It is convenient to define

$$f(q^2, \nu) \equiv \nu^{-1} q^2 (a_1 + q^2 a_2) \quad (E.4)$$

which is even in ν . By using the explicit expressions (2.47) and (2.48), one can readily prove that a_1 , a_2 , b and c are all regular at $\nu = 0$. At a fixed q^2 , as $\nu \rightarrow 0$ Eq. (E.3) implies $\nu^{-1} q^2 (a_1 + q^2 a_2) \rightarrow -ibq^2$ which, in turn, on account of (E.2), approaches 2. Thus, one finds that at $\nu = 0$

$$f(q^2, 0) = 2. \quad (\text{E.5})$$

Next, we shall show that at a fixed q^2

$$f(q^2, \nu) \sim 0(\nu^{-2}) \quad \text{as } \nu \rightarrow \infty. \quad (\text{E.6})$$

This can be established by following almost exactly the same arguments used in Appendix D for A_{11} and B_{11} , except that instead of the scaling limit, one now takes the limit of $\nu \rightarrow \infty$ while keeping q^2 fixed. We note that (D.3) remains valid. Since in the laboratory frame $P_\mu = q_\mu + 0(m)$, the numerator on the right hand side of (D.4) remains $0(\nu)$, as before. Thus, (D.4) is $0(m^{-1})$ if $P^2 = 0(m\nu)$, in which case the corresponding integration volume $\int d^4X = 0(m^4)$. If $P^2 = 0(m^2)$, then (D.4) is $0(\nu)$, but the corresponding integration volume is $0(m^5/\nu)$, because of (D.5). Consequently, in the laboratory frame $A_{11}(p, q)$ is finite in the limit $\nu \rightarrow \infty$. Furthermore, the same limit holds if $\nu \rightarrow -\infty$. The difference $A_{11}(p, q) - A_{11}(p, -q)$ is, therefore, $0(\nu^{-1})$. Similar arguments and conclusions can be readily extended to the differences $A_{33}(p, q) - A_{33}(p, -q)$, $B_{11}(p, q) - B_{11}(p, -q)$ and $B_{33}(p, q) - B_{33}(p, -q)$. By using (2.54), (2.57) and (E.3), one establishes the asymptotic condition (E.6).

Since $f(q^2, \nu)$ is an even function in ν , one may consider the complex

$z = v^2$ plane, and regard f as a function of z , keeping q^2 fixed. In this complex plane, f has a pole at

$$z = v_o^2 \equiv [q^2/(2m_p)]^2 \quad (E.7)$$

and a cut along the real axis extending from v_{\min}^2 to ∞ where

$$v_{\min} = (2m_p)^{-1} [q^2 + (M + \mu)^2 - m_p^2] \quad (E.8)$$

To study the discontinuity of f across the cut, it is only necessary to investigate the absorptive part of $F'_{\lambda v}$ for $v > 0$. By using (2.47) and (2.48), one sees that for $v > 0$ the absorptive parts of $F'_{\lambda v}$ and $F_{\lambda v}$ are equal where $F_{\lambda v}$ is the forward Compton amplitude defined by (2.46). It follows then that the discontinuity of f across the cut is simply $2i \operatorname{Im}(v U_2)$ where U_2 is defined by (2.51). The standard Cauchy theorem and the asymptotic condition (E.6) lead to, for z away from these singularities,

$$f(q^2, z) = f(q^2, v_o^2) + \pi^{-1} \int_{v_{\min}^2}^{\infty} dv^2 (v^2 - z)^{-1} \operatorname{Im}(v U_2) \quad (E.9)$$

Upon setting $z = 0$ and changing the variable v to $x = q^2/(2m_p v)$ while keeping q^2 fixed, (E.9) becomes, on account of (E.5),

$$1 = \frac{1}{2} f(q^2, v_o^2) + \pi^{-1} \int_0^{x_{\max}} x^{-1} dx \operatorname{Im}(v U_2) \quad (E.10)$$

where $x_{\max} = 1 - q^{-2} [(M + \mu)^2 - m_p^2]$. By repeating exactly the same argument used in the preceding Appendix, one can show that (2.52) can also be written, at a fixed x , as

$$\operatorname{Im}(v U_2) = \pi (v W_2) [1 + O(m^2 q^{-2})] \quad .$$

As $q^2 \rightarrow \infty$, one has $f(q^2, v_o^2) \rightarrow 0$ since it is proportional to the square of the elastic electromagnetic form factor. Moreover, $x_{\max} \rightarrow 1$ and at fixed x

$$\text{Im}(v U_2) \rightarrow \pi(v W_2) ;$$

(E. 10) becomes then simply the Adler sum rule (2.53).

References

1. J. D. Bjorken, Phys. Rev. 179, 1547 (1969). R. P. Feynman (unpublished); Phys. Rev. Letters 23, 1415 (1969); Proceedings of the Third International Conference on High Energy Collisions at Stony Brook (Gordon and Breach, New York, 1969). J. D. Bjorken and E. A. Paschos, Phys. Rev. 185, 1975 (1969).
2. E. D. Bloom et al., Proceedings of the XVth International Conference on High Energy Physics, Kiev (1970). Henry W. Kendall, report to the 1971 International Symposium on Electron and Proton Interactions at High Energies, Cornell University. See also various references mentioned in these papers.
3. For simplicity, let us assume that in the infinite momentum frame the 3-momentum \underline{k} of the parton is parallel to the 3-momentum \underline{p} of the physical proton; i.e., in the frame $\underline{p} \rightarrow \infty$, $\underline{k} = x \underline{p}$. Therefore, one may write for the 4-momentum $k_\lambda = x p_\lambda + 0(|\underline{p}|^{-1})$. In the evaluation of the vW_2 function, in order to replace $\delta(q^2 + 2k \cdot q)$ by $\delta(q^2 + 2xp \cdot q)$, one must have either the time component q_0 of the virtual photon to remain finite as $\underline{p} \rightarrow \infty$, or the difference $k_\lambda - x p_\lambda$ to be zero identically [not just $0(|\underline{p}|^{-1})$]. The former restricts the direction \underline{p} of the infinite momentum frame, and the latter implies that the parton has no strong interaction and, furthermore, it is of mass $x m_p$ where m_p denotes the proton mass.
4. Sidney D. Drell and Tung-Mow Yan, Ann. of Physics 66, 578 (1971).

5. Y. S. Tsai (unpublished); R. Jackiw and G. Preparata, Phys. Rev. Letters 22, 975 (1969); S. L. Adler and Wu-Ki Tung, Phys. Rev. Letters 22, 978 (1969).
6. See, e.g., S. D. Drell, Donald J. Levy and Tung-Mow Yan, Phys. Rev. 187 2159 (1969); D1, 1035, 1617 (1970).
7. See, e.g., S. B. Treiman and D. Gross (Princeton University preprint).
8. The electromagnetic radiative corrections are known to introduce deviations from the scaling property $\sim 0 (\alpha \ln q^2)$. The question whether there might be similar deviations due to non-electromagnetic radiative corrections associated with meson fields is, as yet, an open one. As we shall see in the following sections, at least in the ladder approximation of the Bethe-Salpeter equation, the scaling property can be shown to hold rigorously for a large class of relativistic field theories. [See comment E in section V for further discussions.]
9. For parton models based on quarks as constituents, see J. D. Bjorken and E. Paschos, loc. cit., and J. Kuti and V. F. Weisskopf, Phys. Rev. (in press).
10. J. S. Ball and F. Zachariasen, Phys. Rev. 170, 1541 (1968); D. Amati, L. Caneschi and R. Jengo, Nuovo Cimento 58, 783 (1968); D. Amati, R. Jengo, H. R. Rubinstein, G. Veneziano and M. A. Virasoro, Phys. Letters 27B, 38 (1968); M. Ciafaloni and P. Menotti, Phys. Rev. 173, 1575 (1968); M. Ciafaloni, Phys. Rev. 176, 1898 (1968).
11. A linear $(1-x)$ dependence is obtained by Bjorken and Paschos (loc. cit.) for their three-quark model. The same linear dependence is also obtained by Drell, Levy and Yan (loc. cit.) in their field-theoretical calculation with an ad hoc transverse momentum cut-off.

12. S. D. Drell and Tung-Mow Yan, Phys. Rev. Letters 24, 181 (1970). Cf. G. B. West, Phys. Rev. Letters 24, 1206 (1970). See also the comment below Eq. (4.39) in section IV.
13. There exists a substantial amount of literature on the Bethe-Salpeter equation.
 Among the early ones are E. Salpeter and H. Bethe, Phys. Rev. 84, 1232 (1951); M. Gell-Mann and F. Low, Phys. Rev. 84, 350 (1951); G. C. Wick, Phys. Rev. 96, 1124 (1954); R. Cutkosky, Phys. Rev. 96, 1135 (1954); S. Mandelstam, Proc. Roy. Soc. (London) A233, 248 (1955); A. Klein and C. Zemach, Phys. Rev. 108, 126 (1957); R. Blankenbecler and L. F. Cook, Jr., Phys. Rev. 119, 1745 (1960); R. E. Cutkosky and M. Leon, Phys. Rev. 135, B1445 (1964). For further references, see, e.g., those given by C. H. Llewellyn Smith, Nuovo Cimento 60A, 348 (1969).
14. Throughout the paper, we adopt the convention that $d^4k = d^3\underline{k} dk_0$, the scalar product between any two 4-vectors, say k_ν and q_ν , is $k \cdot q = \underline{k} \cdot \underline{q} - k_0 q_0$, and the Dirac γ -matrices are all Hermitian. For the time-reversal operation used in Eq. (2.13) below, these γ -matrices are assumed to be explicitly given by the usual Pauli representation: $\gamma_1 = \rho_2 \sigma_1$, $\gamma_4 = \rho_3$ and therefore $\gamma_5 = -\rho_1$ where ρ_i and σ_i each represents a set of the usual three Pauli matrices.
15. See also the discussions given by J. F. Ball and F. Zachariasen, loc. cit., and by D. Amati et al., loc. cit.
16. R. E. Cutkosky and M. Leon, loc. cit.
17. S. L. Adler, Phys. Rev. 143, 1144 (1966); see also J. D. Bjorken, Phys. Rev. 148, 1467 (1966).
18. See rapporteurs talk, "Lepton-Hadron Interactions and Quantum Electrodynamics", by Richard Wilson to the XV Annual Conference on High Energy Physics, Kiev, 1970.

19. For discussions of the non-relativistic problem, c.f. S. D. Drell, A. Finn and M. H. Goldhaber, Phys. Rev. 157, 1402 (1967).
20. G. C. Wick, loc. cit.
21. R. E. Cutkosky, loc. cit.
22. See in particular the analyses of Amati et al., Ref. 10.
23. J. D. Walecka and P. A. Zucker, Phys. Rev. 167, 1479 (1968); P. L. Pritchett, J. D. Walecka and P. A. Zucker, Phys. Rev. 184, 1825 (1969); P. L. Pritchett and P. A. Zucker, Phys. Rev. D1, 175 (1970).
24. J. D. Bjorken, Phys. Rev. D1, 1376 (1970); J. Kuti and V. F. Weisskopf, to be published.
25. M. G. Doncel and E. de Rafael, IHES preprint (1971); F. Niedermayer, Eötvös University Thesis (1971); L. Gálfi, P. Gnädig, J. Kuti, F. Niedermayer and A. Patkós, paper presented at the Kiev Conference (1970); ITP-Budapest report no. 281 (1971), paper to be published.
26. P. V. Landshoff, J. C. Polkinghorne and R. D. Short, Nuclear Physics B28, 225 (1971).
27. G. B. West, Phys. Rev. Letters 24, 1206 (1970).
28. See, e.g., E. Jahnke and F. Emde, Tables of Functions (New York, Dover Publications, 1945), 4th edition.

Captions

- Figure 1. Graphical representation of the Bethe-Salpeter equation for the bound-state wave function $\phi_p(k)$ and its conjugate $\bar{\phi}_p(k)$. [See Eqs. (2.6) and (2.16).] The dashed line denotes the covariant potential V .
- Figure 2. Diagrams for electromagnetic form factors and the normalization condition (2.22).
- Figure 3. Diagrams for deep inelastic ep scattering for the bound-state solution of a simple Bethe-Salpeter equation. [See Eqs. (2.31) and (2.32).] The dashed line denotes the covariant potential V .
- Figure 4. Diagrams for forward Compton scattering. [See Eqs. (2.47) and (2.48).]
- Figure 5. A diagram for a virtual photon $\rightarrow \bar{p} + \text{anything}$.
- Figure 6. Feynman diagrams for $p \rightarrow p + X^0$ and " γ " + $p \rightarrow p + X^0$, assuming that the physical proton is an elementary particle instead of a bound-state composite. [See Eqs. (3.10), (3.11) and (3.14).]
- Figure 7. Diagrams for deep inelastic ep scattering in the simple phenomenological model calculation. [See Eqs. (4.4)-(4.7).]
- Figure 8. $2m_p W_1$ versus $\omega = x^{-1}$. The experimental data are taken from Bloom et al., Ref. 2, and the theoretical curve is plotted by using Eq. (4.20) and choosing $\alpha_p = 1.4$ and $\beta_p = 0.22$.

Figure 9. The ratio $(W_1)_n / (W_1)_p$ versus x . The theoretical curve is obtained by using Eqs. (4.20) and (4.27), and choosing $\beta_p = \beta_n$ and $\alpha_p = 1.4$.

Figure 10. A schematic diagram for " γ " + $p \rightarrow p$ + mesons.

$$\begin{aligned}
 \phi_p &= \text{diagram 1} = \text{diagram 2} \\
 \bar{\phi}_p &= \text{diagram 3} = \text{diagram 4}
 \end{aligned}$$

Figure 1 shows four Feynman diagrams. The first two diagrams are for ϕ_p . The first diagram shows a horizontal line with a hatched section on the left, labeled p , which splits into two lines: one labeled X^0 going up-right and one labeled p going down-right. The second diagram is identical but includes a dashed vertical line connecting the two outgoing lines. The next two diagrams are for $\bar{\phi}_p$. The third diagram shows two lines, labeled X^0 (top-left) and p (bottom-left), meeting at a vertex that connects to a horizontal line labeled p on the right. The fourth diagram is identical but includes a dashed vertical line connecting the two incoming lines.

Figure 1

$$\begin{aligned}
 \langle p' | J_\nu | p \rangle &= \text{diagram 5} \\
 -i \left[d \ln \lambda / d m_p \right]^{-1} &= \text{diagram 6}
 \end{aligned}$$

Figure 2 shows two Feynman diagrams. The first diagram, corresponding to $\langle p' | J_\nu | p \rangle$, is a bubble diagram. It has two external horizontal lines: the left one is labeled p and has a hatched section, and the right one is labeled p' and also has a hatched section. The bubble consists of two curved lines. The top curve is labeled X^0 and has an arrow pointing right. The bottom curve is labeled p and has an arrow pointing left. A wavy line labeled q with an arrow pointing up connects the two curves. The second diagram, corresponding to $-i [d \ln \lambda / d m_p]^{-1}$, is also a bubble diagram with two external horizontal lines labeled p (left, hatched) and p (right, hatched). The top curve is labeled X^0 with a right-pointing arrow, and the bottom curve is labeled p with a left-pointing arrow.

Figure 2

$$I_\nu = \text{diagram} \quad I'_\nu = \text{diagram}$$

The first diagram shows a horizontal line with a hatched section on the left, labeled p . From the right end of this line, two lines branch out: one goes up and to the right, labeled X , and the other goes down and to the right, labeled P . A wavy line labeled q enters from the bottom and connects to the lower branch.

The second diagram is similar but includes a box labeled T . The horizontal line is labeled p . The upper branch is labeled X' and the lower branch is labeled P' . Both branches enter a box labeled T . From the right side of the box, two lines emerge: one labeled X and one labeled P . A wavy line labeled q enters from the bottom and connects to the lower branch.

where

$$\text{diagram} = \text{diagram} + \text{diagram} + \dots$$

The first diagram on the right is a box labeled T with four horizontal lines entering from the left: the top one is labeled X' and the bottom one is labeled P' . Two horizontal lines exit from the right: the top one is labeled X and the bottom one is labeled P . Two vertical lines connect the top and bottom horizontal lines inside the box.

The second diagram is identical to the first, but the two vertical lines inside the box are dashed.

Figure 3

$$A_{\lambda\nu}(p, q) = \text{diagram}$$

The diagram shows a circle with a hatched section on the left, labeled p , and a hatched section on the right, labeled P . The top of the circle has an arrow pointing right, labeled X . The bottom of the circle has two wavy lines entering: the left one is labeled q and λ , and the right one is labeled q and ν . The label P is also placed below the circle.

$$B_{\lambda\nu}(p, q) = \text{diagram}$$

The diagram shows a circle with a hatched section on the left, labeled p , and a hatched section on the right, labeled P . The top of the circle has an arrow pointing right, labeled X . The bottom of the circle has two wavy lines entering: the left one is labeled q and λ , and the right one is labeled q and ν . The label P is also placed below the circle. Inside the circle, there is a vertical rectangle labeled T .

Figure 4

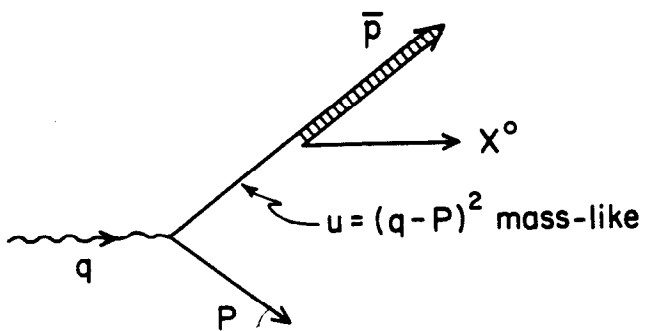


Figure 5

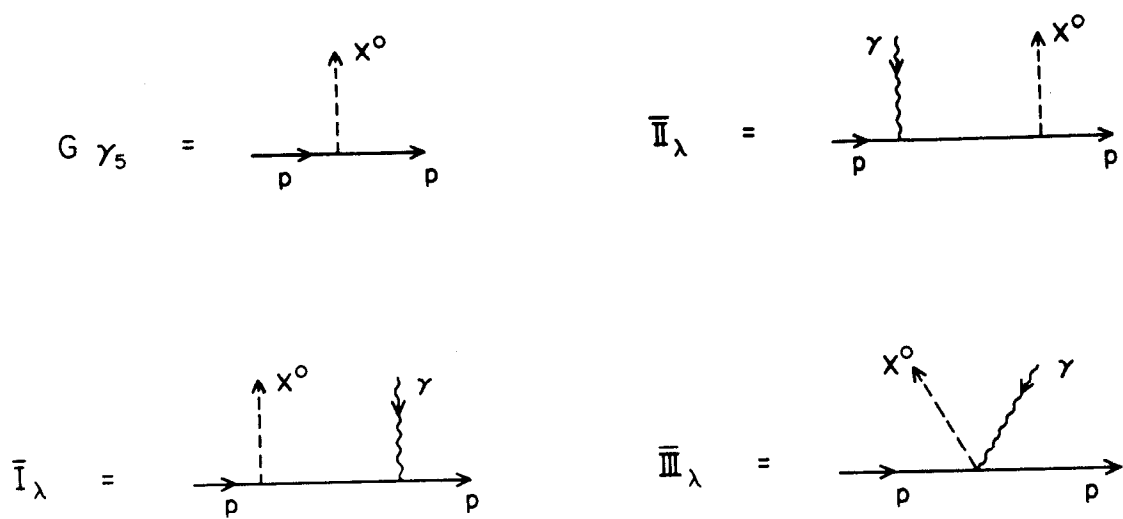


Figure 6

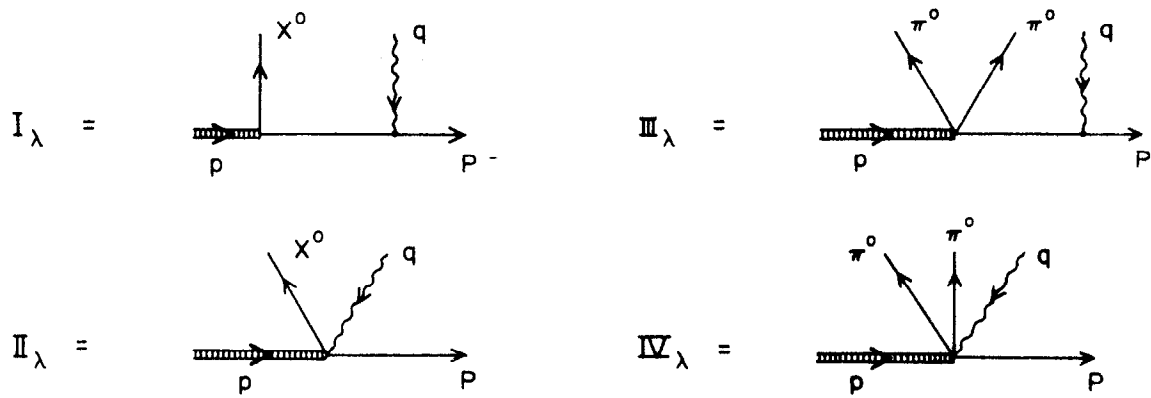


Figure 7

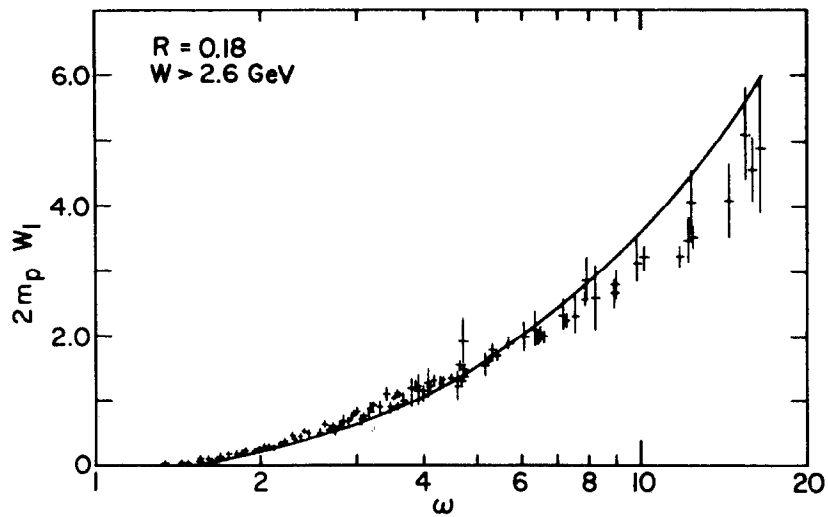


Figure 8

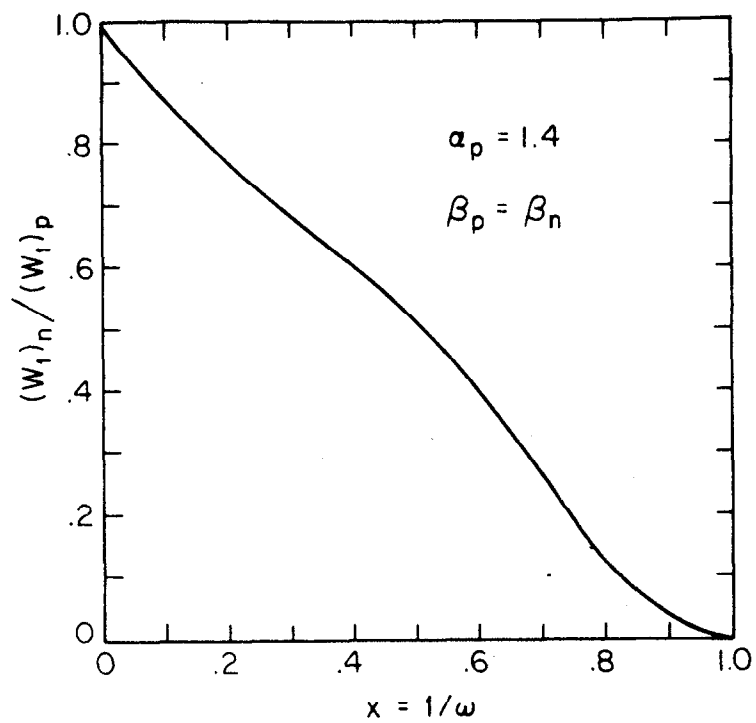


Figure 9

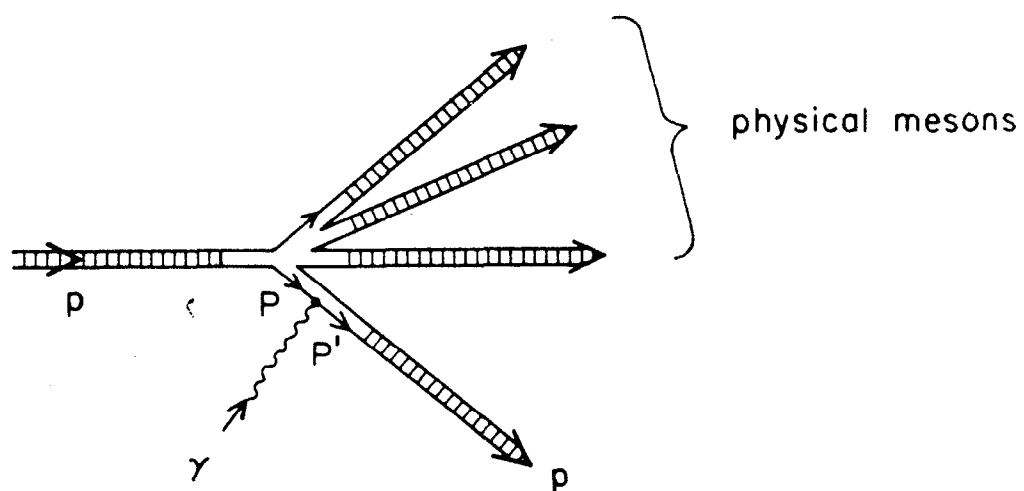


Figure 10